Biogeosciences, 17, 381–404, 2020
https://doi.org/10.5194/bg-17-381-2020

Biogeosciences Open Access EGU

Trace element composition of size-fractionated suspended particulate matter samples from the Qatari Exclusive Economic Zone of the Arabian Gulf: the role of atmospheric dust

Oguz Yigiterhan[1], Ebrahim Mohd Al-Ansari[1], Alex Nelson[2], Mohamed Alaa Abdel-Moati[3], Jesse Turner[2], Hamood Abdulla Alsaadi[1], Barbara Paul[2], Ibrahim Abdullatif Al-Maslamani[4], Mehsin Abdulla Al-Ansi Al-Yafei[5], and James W. Murray[2]

[1]Environmental Science Center, Qatar University, P.O. Box 2713, Doha, State of Qatar
[2]School of Oceanography, University of Washington, Seattle, WA 98195-5351, USA
[3]Environmental Assessment Department, Ministry of Municipality and Environment, P.O. Box 39320, Doha, State of Qatar
[4]Office of Vice President for Research and Graduate Studies, Qatar University, P.O. Box 2713, Doha, State of Qatar
[5]Department of Biological and Environmental Sciences, Qatar University, P.O. Box 2713, Doha, State of Qatar

Correspondence: Oguz Yigiterhan (oguz@qu.edu.qa)

Received: 12 May 2019 – Discussion started: 17 May 2019
Revised: 15 November 2019 – Accepted: 2 December 2019 – Published: 27 January 2020

Abstract. We analyzed net-tow samples of natural assemblages of plankton, and associated particulate matter, from the Exclusive Economic Zone (EEZ) of Qatar in the Arabian Gulf. Size-fractionated suspended particles were collected using net tows with mesh sizes of 50 and 200 µm to examine the composition of small- and large-size plankton populations. Samples were collected in two different years (11 offshore sites in October 2012 and 6 nearshore sites in April 2014) to examine temporal and spatial variabilities. We calculated the excess metal concentrations by correcting the bulk composition for inputs from atmospheric dust using aluminum (Al) as a lithogenic tracer and the metal/Al ratios for average Qatari dust. Atmospheric dust in Qatar is depleted in Al and enriched in calcium (Ca), in the form of calcium carbonate ($CaCO_3$), relative to the global average Upper Continental Crust (UCC). To evaluate the fate of this carbonate fraction when dust particles enter seawater, we leached a subset of dust samples using an acetic acid–hydroxylamine hydrochloride (HAc–HyHCl) procedure that should solubilize $CaCO_3$ minerals and associated elements. As expected, we found that Ca was removed in Qatari dust; however, the concentrations (ppm) for most elements actually increased after leaching because the reduction in sample mass resulting from the removal of $CaCO_3$ by the leach was more important than the loss of metals solubilized by the leach. Because surface seawater is supersaturated with respect to $CaCO_3$ and acid-soluble Ca is abundant in the particulate matter, we only used unleached dust for the lithogenic correction. Statistical analysis showed that for many elements the excess concentrations were indistinguishable from zero. This suggested that the concentrations of these elements in net-tow plankton samples were mostly of lithogenic (dust) origin. These elements include Al, Fe, Cr, Co, Mn, Ni, Pb, and Li. For several other elements (Cd, Cu, Mo, Zn, and Ca) the excess concentrations present after lithogenic correction are most likely of biogenic/anthropogenic origin. The excess concentrations, relative to average dust, for most elements (except Cd) decreased with distance from the shore, which may be due to differences in biology, currents, proximity to the coast, or interannual processes.

1 Introduction

There have been few trace metal analyses carried out in coastal environments and marginal seas such as the Arabian Gulf (Bu-Olayan et al., 2001; Khudhair et al., 2015). Data for the major and trace elemental composition of marine particulate matter are essential for our understanding of biogeochemical cycling in the ocean. Identification of the biotic

fraction is made complicated by the heterogeneity of particle assemblages. In most areas of the open ocean marine particles are mostly composed of phytoplankton and zooplankton (e.g., Krishnaswami and Sarin, 1976; Collier and Edmond, 1984). Their composition is influenced by a variety of processes that include active uptake by phytoplankton, grazing by zooplankton, adsorption–desorption, particle aggregation, and microbial remineralization (e.g., Turekian, 1977; Bruland and Franks, 1983; Bruland et al., 1991; Alldredge and Jackson, 1995). However, in the open ocean (e.g., Dammshauser et al., 2013; Rauschenberg and Twining, 2015; Ohnemus and Lam, 2015), and especially in marginal seas and coastal regions, lithogenic, abiotic particles are also important (Collier and Edmond, 1984; Twining et al., 2008; Iwamoto and Uematsu, 2014; Ho et al., 2007). These abiotic particles can include lithogenic minerals that are input from rivers, atmospheric dust, and sediment resuspension as well as authigenic particles such as Fe and Mn oxyhydroxides. The relative contributions of biotic and abiotic particles can differ significantly. In some cases, the trace element contents of abiotic material can dominate the total composition (e.g., Ho et al., 2007). Distinguishing biogenic versus abiotic elemental composition is complicated. There have been few studies that tried to distinguish the relative contributions of biotic and abiotic particles in marine particulate matter (Lam et al., 2015; Ohnemus and Lam, 2015; Ohnemus et al., 2017; Wen-Hsuan Liao et al., 2017). Biogenic and abiotic particles are difficult to separate physically using most bulk sampling techniques. Characterizing the composition of biogenic particles is difficult due to the difficulties associated with sampling techniques and analyses (Martin and Knauer, 1973; Collier and Edmond, 1984; Ho et al., 2003; Twining et al., 2004; Rauschenberg and Twining, 2015). Bulk chemical analyses can be used to determine the relative contributions when the compositions of the end-members are known. There can be significant differences in composition spatially and among species of phytoplankton, making regional inferences difficult to evaluate when considering only average data sets. The biogenic portion can be determined after correcting for the lithogenic portion of the total concentration, using metal to aluminum ratios (Me/Al) and assuming Al as the lithogenic tracer (Bruland et al., 1991; Ho et al., 2007; Yigiterhan et al., 2011, 2018). Metal to phosphorus (Me/P) ratios have been used as a way to normalize comparison of the biogenic portion of data sets from studies from different locations (Yigiterhan et al., unpublished data, 2020) using different sampling techniques (e.g., Knauer and Martin, 1981; Kuss and Kremling, 1999). Ho et al. (2007) used a combined Me/Al and Me/P approach to suggest that most of the trace metals associated with plankton, in samples from the coastal and open South China Sea, were associated with extracellular abiotic (inorganic) particles of atmospheric origin.

Particulate matter in seawater contains an important reservoir that can be solubilized and made biologically available. Some researchers have developed selective chemical leach approaches to identify labile trace metals. No chemical leach technique will be able to perfectly mimic natural processes, but some have attempted to preferentially extract trace metals that are associated with intracellular material and particles adsorbed only to cells (e.g., Sañudo-Wilhelmy et al., 2001; Twining et al., 2011). The acetic acid–hydroxylamine (HAc–HyHCl) leach with a short heating step, developed by Berger et al. (2008), was designed to identify the fraction of trace metals associated with cellular material and labile metals that may be adsorbed or associated with authigenic Mn/Fe oxyhydroxides, which might be available to plankton. The element stoichiometries of individual cells can be determined using synchrotron-based X-ray fluorescence (SXRF), ensuring accurate particulate measurements to ascertain biotic origin (Twining et al., 2003, 2004). However, though surprisingly inexpensive, SXRF is time-consuming and not always accessible, resulting in limited sample throughput. All approaches to distinguish biotic and abiotic compositions have advantages and disadvantages. A systematic comparison of different methods was conducted by Rauschenberg and Twining (2015). They concluded that the Berger et al. (2008) leach was the best approach for quantifying biotic and associated labile particulate phases likely to be involved in marine biogeochemical cycling.

The area of our study was the Qatari Exclusive Economic Zone (EEZ), which is located at the center of the Arabian/Persian Gulf (hereafter "the Gulf"). This region is heavily impacted by atmospheric dust, massive construction, sediment dredging, heavy industrialization, oil and gas exploitation, marine transportation, and desalination plants, which renders it an ideal location to examine the influence of these coastal processes on particulate trace element compositions (Barlett, 2004; Richer, 2009; Al-Ansari et al., 2015; Jish Prakash et al., 2015; Yigiterhan et al., 2018). As there are essentially no rivers, atmospheric dust deposition is the main source of lithogenic particles to the surface marine waters of the Gulf. We examined the composition of local atmospheric dust in Qatar (Yigiterhan et al., 2018) and compared it with average Upper Continental Crust (UCC; Rudnick and Gao, 2003) and local surface terrestrial deposits (TSD, Yigiterhan et al., 2018) to determine the legitimacy of using each for a lithogenic correction. The aeolian dust in Qatar is rich in Ca (as potentially soluble $CaCO_3$ and $CaSO_4$ minerals), and this complicates the use of Al as a tracer for the lithogenic correction. We studied the effect of distance from the shore on the elemental concentrations in small- and large-size fractions of net-tow particulate matter in coastal seawater samples, with the goal of determining the influence of dust, plankton, and anthropogenic sources in the Qatar EEZ.

2 Methods

The technique used in this study involved analyzing the total composition of bulk samples collected using net tows of natural plankton assemblages. A subset of previously collected dust samples was leached using a modified version of the acetic acid–hydroxylamine hydrochloride procedure of Berger et al. (2008). The apparent excess concentrations (biogenic plus anthropogenic) in the net-tow samples were determined by correcting for the lithogenic portion of the total concentration, using aluminum as the lithogenic tracer (Bruland et al., 1991; Ho et al., 2007; Yigiterhan et al., 2011) and the average composition of Qatari dust. This procedure provides an estimate of the non-lithogenic portion and includes labile elements that may be part of and available to plankton.

2.1 Study region

The Arabian/Persian Gulf is a 1000 km long and 338 km wide arm of the Indian Ocean (Arabian Sea), covering 233 100 km^2 in area. The basin is semi-enclosed and shallow with an average depth of 36 m. It is one of the hottest, driest, most saline, and dustiest areas on earth. In most of the Gulf seawater salinities range from 37 to 41. The Gulf is characterized by reverse flow and estuarine circulation (in at the surface and out at depth) with no sill or saddle restriction at the southern entrance in the Strait of Hormuz (Reynolds, 1993; Swift and Bower, 2003). The first comprehensive description of the region's hydrographic properties, nutrients, and carbonate chemistry was presented by Brewer and Dyrssen (1985). They reported the following.

1. Strong south-to-north salinity gradients exist in the Gulf, with salinities greater than $S = 40$ to the north.

2. Low nutrient levels everywhere in the surface waters, except for the surface inflow from the Gulf of Oman through the Strait of Hormuz.

3. The ratio of carbon fixed as $CaCO_3$ to organic carbon, fixed during biological production, was about 2.5 to 1.

While there is a paucity of published data on primary productivity and diversity of phytoplankton in the region, existing information reveals north-to-south trends (Rao and Al-Yamani, 1998; Dorgham, 2013; Polikarpov et al., 2016) which are driven by particular environmental features (e.g., eutrophication, dust input, and coastal (shallow) versus open (deep) water). Phytoplankton biomass (chlorophyll *a* concentration), primary production, abundance, species diversity, and species groupings, together with water quality parameters, were measured in the Qatari EEZ by Quigg et al. (2013). Of the 125 species identified, 70 % to 89 % were diatoms (mainly *Chaetoceros*), 8 % to 22 % were dinoflagellates, and the remaining 2 % to 6 % were cryptophytes. No coccolithophorids were identified.

2.2 Sample collection

Particulate matter samples were obtained during three separate expeditions in the Exclusive Economic Zone (EEZ) of Qatar. The first expedition was conducted on the R/V *Janan* from 13 to 14 October 2012 and included 11 sampling sites in the Qatar EEZ, located at the east of the Qatar Peninsula (Fig. 1). Sampling locations were selected to include samples from nearshore sites (Khor Al-Odaid, Mesaieed, Dukhan, Umm Bab) to offshore sites (Shraawoo's Island, Al-Edd Al-Sharqi (Ash Sharqi), Al-Edd Al-Gharbi, Halul Island, and High North), along with varying proximity to industrial and urban areas. Some sites, such as Al-Khor and Khor Al-Odaid, are adjacent to environmentally protected areas in Qatar, while others, such as Mesaieed, Ras Laffan, Dukhan, and Doha, are subject to more industrial influence (Richer, 2009) and urbanization. Doha Bay is a major source of particles to the adjacent Gulf due to intense human activity in the capital city and associated suburbs. Dredging, effluent discharges, extensive construction activities, and heavy traffic are major sources of particulate loading to the bay (Yigiterhan et al., 2018; Alfoldy et al., 2019). The water maximum bottom depth range for 2012 sampling stations varied between 12 and 58 m depth.

The second expedition was conducted using speedboats on 1 to 2 April 2014. Sampling sites were located west of Dukhan, an oil-producing region on the western coast (Dukhan Bay, Fig. 2a), and in shallow waters adjacent to the city of Doha on the eastern coast (Doha Bay, Fig. 2b). At each location, size-fractionated, duplicate, net-tow samples were collected at three stations with increasing distance from the coast along a relatively straight bearing. Sites were selected to investigate how industrialization and coastal processes influence nearshore elemental concentrations on the western and eastern sides of the Qatar Peninsula, where marine waters exhibit different physical and chemical properties. The sampling depths varied between 2 and 5 m in quite shallow bay areas.

Additional sets of samples were collected during a third cruise from offshore locations in October 2014. The sampling was conducted using R/V *Janan* on a linear transect at six stations from the exit of the Doha channel to the border of the EEZ of Qatar. The data from these samples will be used in a later publication (Yigiterhan et al., unpublished data, 2020).

2.3 Sampling

Samples were collected at all locations using custom-designed plankton net tows with mesh sizes of 50 µm (small size fraction) and 200 µm (large size fraction) to examine size-fractionated particulate matter. All sample sets were collected using nets towed horizontally at 1 to 2 m depth at 1.5 knot speed for 10 min ($\sim$ 0.5 km distance). Both samples certainly contained variable assemblages of phytoplankton,

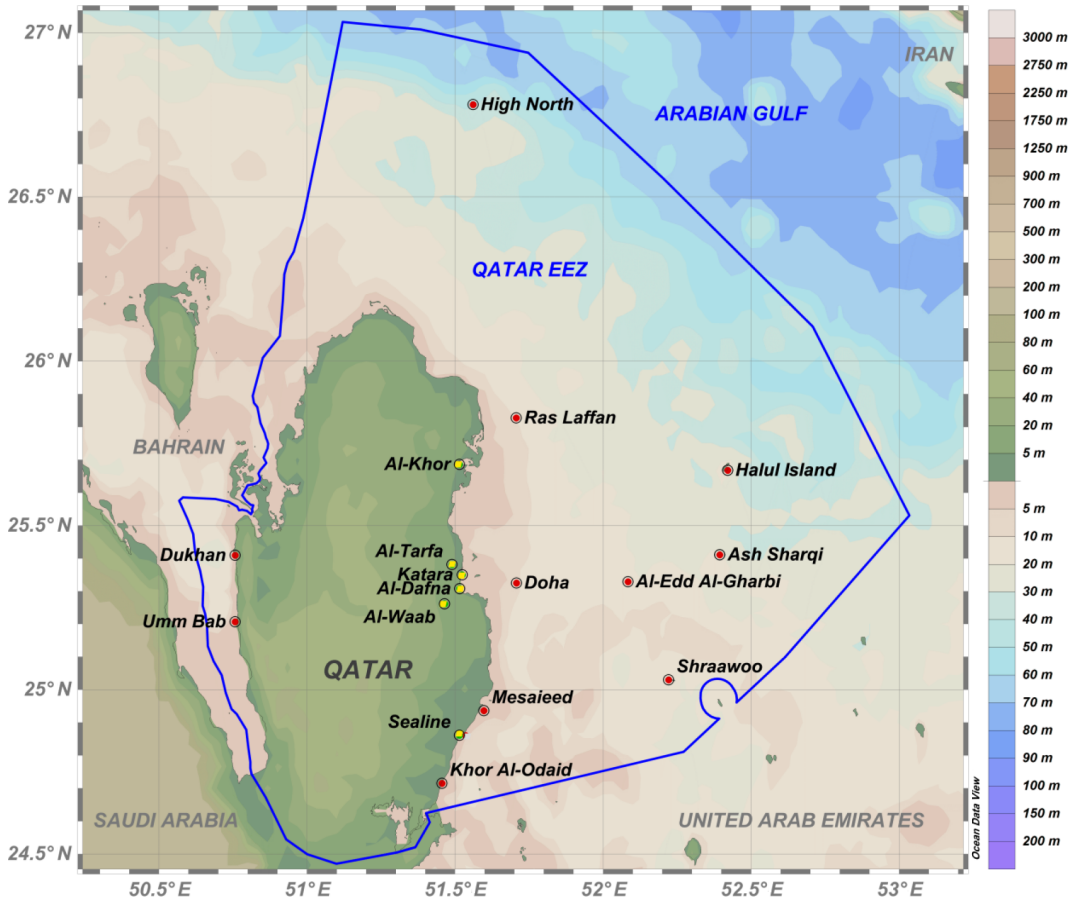

Figure 1. Plankton sampling locations (red dots) for the offshore sampling cruise in October 2012. The land-based sampling stations for atmospheric dust are shown with yellow dots. The Ocean Data View (ODV) program was used for plotting the figure (Schlitzer, 2018).

zooplankton, a small fraction of other planktonic organisms, and terrestrial particles of atmospheric origin (e.g., dust); however, no attempt was made to visually determine their proportions. Metal-free plankton ring nets of 200 cm length and 50 cm diameter (aspect ratio 4 : 1) were used to collect these samples. The particulate samples were rinsed into the cod ends with surface seawater and transferred immediately, and onboard and under cover, into new, acid-cleaned 500 mL borosilicate glass jars with Teflon lids (Environmental Sampling Supply; Cutter et al., 2010). Each jar was carefully soaked for 2 d in 25 % HNO_3 and for another 2 d in 10 % HCL, and then rinsed five times with deionized (DI) water. They were also rinsed three times with surface seawater from the same location before filling with samples from the cod end. The glass jars were kept in a cooler under ice and transferred to 4 °C refrigerators onboard the vessel to allow particles to settle in the dark. In the laboratory, within 2 h of collection, the excess seawater was decanted and particulate samples were re-filtered under vacuum onto 142 mm diameter, 1 µm Nuclepore membrane filters. Particles were gently rinsed using double-distilled DI water to remove excess sea salt before transfer to acid-washed 50 mL polypropylene conical tubes (FALCON, Corning brand). The rinsing step was kept short to minimize breakup of fragile plankton (Collier and Edmond, 1984). As a result, some sea salt still remained in the samples. The contribution of sea salt to dry weight and concentrations of Ca, Mg, K, and Sr was corrected using concentrations of Na.

Samples for atmospheric dust ($n = 5$) were collected from various locations around Qatar (Fig. 1, yellow dots on land), using automated and hand-sampling methods. These samples are a subset of the complete data set for Qatar dust analyses presented in Yigiterhan et al. (2018). Dust accumulation is usually extensive, so collecting dust is very straightforward, but was conducted carefully to avoid contamination. Most individual dust samples were collected over 2- to 4-week intervals. The sampling was done using passive dust traps (Siap + Micros). The particles were collected in an acid-cleaned glass bowl, which has automated protection from the rain with a digitally controlled closing–opening system, activated with rain sensors, for both dry and wet deposition. These traps were regularly visited during the non-stormy autumn and winter seasons from September 2013 to February 2014. Sufficient dust particle accumulation (1 to

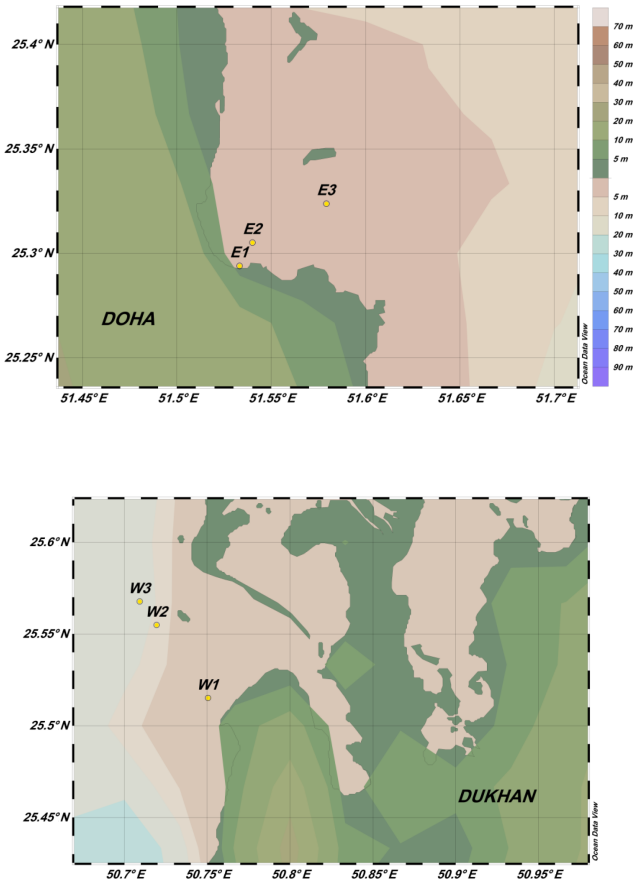

Figure 2. Station locations for the detailed nearshore sampling in April 2014 near Dukhan Bay and Doha Bay. The Ocean Data View (ODV) program was used for plotting the figures (Schlitzer, 2018).

10 g dry weight per container) was achieved after a sampling period of 1 month or more for some stations. When the targeted sample weight was achieved, samples were immediately collected. Sample extraction from the traps was mostly completed over a 48 h period. The dust particles were trapped away from wind and anthropogenic local contaminants. This set of samples was analyzed in total (unleached) and leached forms.

2.4 Sample processing and analyses

The particulate samples, which were previously transferred into conical tubes, were centrifuged for 15 min at ∼ 3000 RPM. Excess water was decanted at the end of the centrifuge cycle and the wet sample weight was recorded. Samples were then kept frozen in the same 50 mL centrifuge tubes at −24 °C until analysis. The frozen samples were desiccated in a freeze drier for 1 week to 10 d before grinding at room temperature using well-cleaned agate mortar and pestle. Trace metal clean techniques were applied during crushing and gently grinding to make a homogenous mixture. The powdered samples were transferred to new, trace metal certified 50 mL polypropylene tubes (UC475-GN – UltimateCup™) to be weighed again for dry weight. These samples were stored at room temperature in a desiccator until acid digestion.

Total acid digestion was completed on a HotBlock (SC154-240, Environmental Express) in acid-cleaned PTFM Teflon™ tubes. A subset of dried, homogenized samples (250 ± 10 mg) was transferred into each tube, followed by addition of reagent grade 1 mL HF (ARISTAR® ULTRA, 48 %, ultrapure), 5 mL HNO_3 (MERCK, 65 %, Ultrapur), and 2.5 mL HCl (Honeywell Fluka™, 37 %, TraceSELECT) to each sample. The temperature of the HotBlock was adjusted carefully, and then tubes were placed on the HotBlock in a fume hood with loose caps at 95 °C for at least 1 h. Addition of trace metal grade acids (HCI and HNO_3) was repeated until a clear digest solution was obtained. Depending on the lipid content of the samples, 1 mL or more of trace metal grade H_2O_2 oxidizer (Riedel-de Haën, 30 %, extra pure, stabilized) was added before further increasing temperature gradually to 135 °C. HotBlock heating continued until near dryness. The sides of the tubes were rinsed consecutively with 1 mL HNO_3 and 5–10 mL of double-distilled deionized (DDI) water. Digests were placed back onto the HotBlock in the fume hood at 155 °C, without using caps, and boiled until clear. Solutions were transferred to new, 50 mL polypropylene tubes (UC475-GN – UltimateCup™) before rinsing the Teflon™ tube and cap at least three times with DDI water. The final sample volume was made up to 50 mL (by volume) by adding more DDI. Samples were stored at room temperature until analysis by an Inductively Coupled Plasma Optical Emission Spectrometer (ICP-OES; PerkinElmer – Optima 7300 DV).

A subset of dust samples was also leached with acetic acid (HAc) and hydroxylamine hydrochloride (HyHCl) with a short heating step to remove more labile particulate concentrations. Dried samples were weighed and then treated with a modification of the leaching process described in Berger et al. (2008). Comparative analyses by Rauschenberg and Twining (2015) and Berger et al. (2008) showed that this technique most effectively digested the biogenic portion while leaving the more refractory elements intact. The leaching solution was composed of Ultra-Pure 25 % acetic acid (pH 2) with 0.02 M hydroxylamine hydrochloride as a reducing agent. The amount of 5 mL of leachate was added to 300 mg of homogenized, desiccated sample in a Nalgene test tube. For some large mesh size samples, less than 300 mg was available, in which case the total sample was used. The test tubes were placed in a beaker of water and raised to a temperature of 95 °C for 10 min, and then left at room temperature for another 2 h before centrifuging at 2500 rpm for 5 min. After the leachate was removed from the sample and discarded, 5 mL of DDI water was added to the tube and shaken vigorously to ensure mixing. Tubes were centrifuged at 2500 rpm for 5 min, after which the water was removed. This rinsing step was performed three times and the leachate

was discarded. The leached and rinsed solid samples were freeze-dried, reweighed, and then totally digested using the procedure described above with the leachable fraction determined by the difference. These samples were also analyzed by ICP-OES to determine the total elemental concentrations.

2.5 Precision and accuracy

Duplicate samples, spiked samples, and certified reference materials (CRMs) supplied by the National Research Council of Canada (NRC) were digested and analyzed twice with each batch of samples (typically 1 in every 10 samples). For precision, three samples were analyzed in duplicate. To ensure accurate measurements, four CRMs were included in the analyses, i.e., PACS-2, PACS-3, MESS-3, and DORM-4. In almost all cases, the average measured values were within the 95 % confidence limits of certified values, and thus the accuracy determined from this approach was comparable to or better than the precision. The limit of detection was defined as 3 times the standard deviation of blank readings.

2.6 Sea salt (sodium) correction

The contribution of sea salt to the total mass and concentrations of elements was corrected using Na as a tracer for sea salt. The correction was done in Eq. (1) as follows:

$$\mathrm{Me}_{\mathrm{corrected}} = \mathrm{Me}_{\mathrm{total}} - \mathrm{Na}_{\mathrm{sample}} \times (\mathrm{Me/Na})_{\mathrm{seawater}}. \quad (1)$$

We used the Me/Na ratios in seawater from Pilson (2013). However, interpreting the correction can be complicated. There is uncertainty in this correction because of our assumption that all Na is from sea salt. The atmospheric dust in this study area is rich in carbonate material. Recent marine carbonate deposits and skeletons have Na concentrations between 2000 and 5000 ppm or between 0.2 % and 0.5 % (Land and Hoops, 1973; Milliman, 1974) and the average Na in our dust samples was 1.89 %. Thus, some of the Na in our marine particulate matter samples could be naturally in the samples, in the form of limestone and dolomite that originated from the aeolian dust (Behrooz et al., 2017). Other major sources of Na in detrital sedimentary rock types are detrital Na-feldspar and clay minerals. For example, the average Na in our un-sea salt corrected particulate samples was 60 000 ppm (or 6 %). But, because the Na varies so much from sample to sample, we decided to use the total Na in each sample for the sea salt correction. If we overestimate the sea salt correction, our sample mass would be too low and the metal concentrations would be too high. However, the magnitude of this uncertainty is within the natural variability, so it can be ignored.

2.7 Lithogenic correction

The total digestion procedure dissolved all abiotic as well as biogenic material in the samples. In order to determine the biogenic portion of the metal concentrations, we used aluminum (Al) as a lithogenic tracer and assumed that all Al in the samples was of lithogenic origin. Aluminum is an effective tracer for lithogenic or terrigenous inputs due to its high crustal abundance and generally little or no biological uptake (Ho et al., 2007). Because river input is absent in the Qatari EEZ, and the underlying sediments are mostly carbonates, we assume that scavenging and biological cycling do not apply for our atmospheric dust and water column samples.

Because the lithogenic samples can consist of materials from different origins, it is best to compare analytical data using Me/Al ratios, rather than absolute metal concentrations to correct for dust contributions (Yigiterhan and Murray, 2008). The Me/Al ratios were calculated for two possible lithogenic materials by dividing the concentration of the desired metal by the Al concentration. For determining lithogenic contributions to our samples, we utilized average total (unleached) Qatari dust (Table 1 in Yigiterhan et al., 2018) and average leached Qatari dust (Table 1, this study). We multiplied these ratios by the Al concentration in each sample to give a value for the lithogenic contribution of each element. After subtracting this value from the total concentrations, the remaining concentration was assumed to be the excess metal ($\mathrm{Me}_{\mathrm{excess}}$) of biogenic, authigenic, or anthropogenic origin (Yigiterhan and Murray, 2008; Yigiterhan et al., 2011). Excess metal concentrations were defined in Eq. (2) as follows:

$$\mathrm{Me}_{\mathrm{excess}} = \mathrm{Me}_{\mathrm{total}} - \mathrm{Al}_{\mathrm{total}} \times \mathrm{Me/Al}_{\mathrm{dust}}. \quad (2)$$

In this study, we only used the unleached dust composition for the lithogenic correction in Tables 2 and 3.

3 Results

3.1 Dust samples

Five dust samples were included in this study. They were analyzed before and after leaching, using the Berger et al. (2008) leaching procedure. The elemental concentration data for the total (unleached) and leached dust samples are reported in Table 1. The goal of this table is to put some limits on the composition of lithogenic particles, originating from terrestrial rocks that are input to the Qatari EEZ from the atmosphere. The total and leached compositions are compared with the global average UCC from Rudnick and Gao (2003) as ratios of total/UCC (column 4) and leached/UCC (column 7). We show this comparison because the UCC is sometimes used for the lithogenic composition when local data sets are not available and we want to show how Qatari dust differs from the UCC. Ratios greater than 1 indicate that the concentrations of elements in these dust samples from Qatar are greater than UCC values. These elements include Ca, Cd, Li, Mg, Mo, Sr, and Zn. As reported previously (Yigiterhan et al., 2018), Qatari dust samples had Ca

Table 1. Average composition of five representative samples of total (strong acid-digested, unleached) Qatari dust, comparison with the average Upper Continental Crust (UCC; Rudnick and Gao, 2003), and composition of leached (total minus labile) Qatari dust. The total and leached compositions are compared with each other and with the UCC as ratios. The unleached and leached compositions are also given as Me/Al ratios. Bold values: calcium (Ca) is the major element of the Qatari dust, which has the highest value in column 4, while having the lowest value in column 6.

Element	Dust $(\text{Total})_{\text{avg}}$ (ppm)	$(\text{UCC})_{\text{R\&G}}$ (ppm)	$(\text{Total})_{\text{avg}}/(\text{UCC})_{\text{R\&G}}$ (ratio)	Dust $(\text{Leached})_{\text{avg}}$ (ppm)	$(\text{D. leached})_{\text{avg}}/(\text{D. total})_{\text{avg}}$ (ratio)	$(\text{Leached})_{\text{avg}}/(\text{UCC})_{\text{R\&G}}$ (ratio)	$(\text{Me/Al})_{\text{total}}$ (ratio)	$(\text{Me/Al})_{\text{leach}}$ (ratio)	$(\text{Me/Al})_{\text{UCC}}$ (ratio)
Al	21 000	81 500	0.26	43 000	2.05	0.53	1	1	1
As	2.08	4.8	0.43	7.01	3.37	1.46	9.90×10^{-5}	1.63×10^{-4}	5.89×10^{-5}
Ba	154	624	0.25	467	3.03	0.75	7.33×10^{-3}	1.09×10^{-2}	7.66×10^{-3}
Be	0.402	2.1	0.19	0.715	1.78	0.34	1.91×10^{-5}	1.66×10^{-5}	2.58×10^{-5}
Ca	137 000	25 700	**5.33**	75 100	**0.55**	2.92	6.52×10^{0}	1.75×10^{0}	3.15×10^{-1}
Cd	0.174	0.09	1.93	0.236	1.36	2.62	8.29×10^{-6}	5.49×10^{-6}	1.10×10^{-6}
Co	5.42	17.3	0.31	9.91	1.83	0.57	2.58×10^{-4}	2.30×10^{-4}	2.12×10^{-4}
Cr	52.6	92	0.57	147	2.79	1.60	2.50×10^{-3}	3.42×10^{-3}	1.13×10^{-3}
Cu	24.7	28	0.88	48.4	1.96	1.73	1.18×10^{-3}	1.13×10^{-3}	3.44×10^{-4}
Fe	11 200	39 200	0.29	26 100	2.33	0.67	5.33×10^{-1}	6.07×10^{-1}	4.81×10^{-1}
K	4260	23 200	0.18	9010	2.12	0.39	2.03×10^{-1}	2.10×10^{-1}	2.85×10^{-1}
Li	38.3	21	1.82	21.4	0.56	1.02	1.82×10^{-3}	4.98×10^{-4}	2.58×10^{-4}
Mg	29 000	15 000	1.93	57 900	2.00	3.86	1.38×10^{0}	1.35×10^{0}	1.84×10^{-1}
Mn	213	775	0.27	290	1.36	0.37	1.01×10^{-2}	6.74×10^{-3}	9.51×10^{-3}
Mo	1.5	1.1	1.36	51.6	34.40	46.91	7.14×10^{-5}	1.20×10^{-3}	1.35×10^{-5}
Na	6550	24 300	0.27	6,370	0.97	0.26	3.12×10^{-1}	1.48×10^{-1}	2.98×10^{-1}
Ni	34.5	47	0.73	211	6.12	4.49	1.64×10^{-3}	4.91×10^{-3}	5.77×10^{-4}
P	310	655	0.47	389	1.25	0.59	1.48×10^{-2}	9.05×10^{-3}	8.04×10^{-3}
Pb	3.64	17	0.21	9.05	2.49	0.53	1.73×10^{-4}	2.10×10^{-4}	2.09×10^{-4}
Sr	775	320	2.42	1100	1.42	3.44	3.69×10^{-2}	2.56×10^{-2}	3.93×10^{-3}
V	39.2	97	0.40	77.3	1.97	0.80	1.87×10^{-3}	1.80×10^{-3}	1.19×10^{-3}
Zn	85.1	67	1.27	212	2.49	3.16	4.05×10^{-3}	4.93×10^{-3}	8.22×10^{-4}

Note: "D." means "Dust".

concentrations 5.3 times larger than in the UCC. Sr(2.4×) > Mg(1.9×) ≥ Cd(1.29×) > Li(1.8×) were also enriched relative to the UCC. Ratios less than 1 suggest that Qatari dust is depleted relative to the UCC. The ratios of leached to total compositions are also included in Table 1 to show the impact of leaching (column 6). The elements removed by the leach have a ratio < 1 and include Ca and Li. All other elements may also be removed but have higher concentrations in the leached material because of the reduction of mass (loss of $CaCO_3$). The total and leached values are also compared using their Me/Al ratios, which is one approach often used for comparing samples with variable compositions (columns 8, 9, 10). Clearly, use of UCC concentrations for the end-member composition of atmospheric dust would not be appropriate for our study because Qatari dust has a large carbonate mineral content reflecting the source regions of Qatar.

3.2 Particulate samples

The elemental compositions of the two size classes of particulate net-tow samples are given in Table 2 (October 2012) and Table 3 (April 2014). The present data are valuable as they represent the first with concentrations of particulate trace elements in the Qatari EEZ. The raw data (column R; Tables 2, 3) for the sea salt corrected composition of the size-fractionated marine particulate matter samples from the 2012 and 2014 cruises are presented by net-tow mesh size. We calculated the lithogenic contributions for each element (column L; Tables 2, 3) using average total (unleached) Qatari dust (from Table 1) and the resulting excess concentrations for each element (column E; Tables 2, 3). Al only has column R as it was used to calculate the lithogenic fraction. Average values and standard deviations for each size fraction are shown in the last row of each section. The cumulative average and standard deviation are shown at the bottom. The data are grouped by filter size with the 50 µm samples at the top and the 200 µm samples at the bottom. For some elements in some samples, the dust correction (L) was larger than the original signal (R), and this resulted in negative values for excess metal (E) concentrations (Tables 2, 3). As negative values are impossible it means that, in some cases, the lithogenic correction done with total (unleached) Qatari dust data overcorrected for the lithogenic input. We treated this as a random error and argued that it is best to focus on the rows with the average and standard deviation for the cumulative (50 + 200 µm) data set for each element.

We also calculated the excess concentrations assuming that the lithogenic fraction had the average values of leached

Table 2. Data for the trace element composition of plankton from the 2012 cruise with average Qatari dust, used for the lithogenic correction. The upper segment shows results for a small-size fraction (phytoplankton), collected with a 50 µm net tow. The lower segment shows data for the large size fraction (zooplankton), collected with a 200 µm net tow. The "Cumulative" row is an average of both of these size fractions. For both size classes and the Cumulative data averages and standard deviations are given. The distance column gives the shortest distance from land to each sampling location (in kilometers). The letters *R*, *L*, and *E* represent the raw data, the lithogenic correction (in this case with average Qatari dust), and the excess concentrations, respectively. All concentrations are parts per million (ppm), or $\mu g\,g^{-1}$. Aluminum only has a raw data column because the entire Al in each sample was assumed to be of lithogenic origin, meaning that the lithogenic correction would be zero. The number in scientific notation in parentheses adjacent to the *L* column is a numerical representation of the [Me]/Al ratio found in Qatari dust (Yigiterhan et al., 2018) used to determine the lithogenic correction. Certain elements have excess values, which are negative, indicating that there was an overcorrection for the lithogenic portion of the sample.

	Bulk plankton (50 µm)		Al	As			Ba			Cd			Co			Cr			Cu		
Sample no.	Location	Distance (km)	*R*	*R*	*L*	*E*	*R*	*L*	*E*	*R*	*L*	*E*	*R*	*L*	*E*	*R*	*L*	*E*	*R*	*L*	*E*
1	Doha	10.19	2592	31.4	0.26	31.2	14.1	18.97	−4.92	0.52	0.02	0.50	1.18	0.67	0.51	6.31	6.49	−0.18	9.3	3.04	6.2
2	Khor Al-Odaid	0.23	994	13.2	0.10	13.1	5.7	7.27	−1.59	1.01	0.01	1.00	1.00	0.26	0.75	3.72	2.49	1.23	10.4	1.17	9.2
3	Mesaieed	0.60	3013	8.6	0.30	8.3	17.9	22.05	−4.11	0.64	0.02	0.62	1.14	0.78	0.37	11.59	7.54	4.05	183.7	3.54	180.2
4	Shraawoo	59.60	1943	13.9	0.19	13.7	14.7	14.22	0.48	1.11	0.02	1.09	0.96	0.50	0.46	5.21	4.86	0.35	82.3	2.28	80.1
5	Al-Edd Al-Gharbi	46.55	480	6.6	0.05	6.5	53.4	3.52	49.84	0.81	0.00	0.81	0.52	0.12	0.39	1.20	1.20	0.00	10.8	0.56	10.2
6	Ash Shargi Oilfield	78.90	1830	9.2	0.18	9.0	26.8	13.39	13.36	2.71	0.02	2.70	0.95	0.47	0.48	6.40	4.58	1.82	41.4	2.15	39.3
7	Halul Island	84.05	1026	10.9	0.10	10.8	12.4	7.51	4.88	3.59	0.01	3.58	1.02	0.26	0.76	8.51	2.57	5.94	13.9	1.21	12.7
8	High North	74.55	1182	12.2	0.12	12.1	6.6	8.65	−2.02	2.03	0.01	2.02	0.88	0.30	0.57	3.71	2.96	0.75	11.2	1.39	9.8
9	Ras Laffan	11.40	803	16.1	0.08	16.1	5.5	5.88	−0.33	1.56	0.01	1.56	0.52	0.21	0.31	4.00	2.01	1.99	56.9	0.94	56.0
10	Dukhan	0.02	10524	28.5	1.04	27.5	69.5	77.02	−7.49	0.36	0.09	0.27	3.00	2.71	0.29	24.87	26.35	−1.49	11.9	12.36	−0.5
11	Umm Bab	0.48	7227	19.3	0.72	18.6	42.5	52.89	−10.43	0.55	0.06	0.49	2.38	1.86	0.52	17.59	18.10	−0.51	12.6	8.49	4.1
	Average		2874	15.4		15.2	24.5		3.42	1.35		1.33	1.23		0.49	8.47		1.27	40.4		37.0
	2× SD		6304	16.1		15.7	43.0		33.28	2.06		2.09	1.53		0.31	14.13		4.28	106.7		107.6
	Zooplankton (200 µm)		*R*	*R*	*L*	*E*	*R*	*L*	*E*	*R*	*L*	*E*	*R*	*L*	*E*	*R*	*L*	*E*	*R*	*L*	*E*
12	Doha	10.19	3,253	17.9	0.32	17.6	16.9	23.80	−6.86	0.70	0.03	0.68	1.17	0.84	0.33	8.96	8.14	0.82	12.9	3.82	9.1
13	Khor Al-Odaid	0.23	1012	8.4	0.10	8.3	6.1	7.40	−1.34	1.17	0.01	1.17	1.30	0.26	1.04	3.07	2.53	0.54	9.8	1.19	8.6
14	Mesaieed	0.60	2774	7.6	0.27	7.4	11.8	20.30	−8.54	0.63	0.02	0.60	1.93	0.72	1.21	11.87	6.95	4.92	14.1	3.26	10.8
15	Shraawoo	59.60	722	10.7	0.07	10.6	4.8	5.28	−0.52	0.78	0.01	0.78	0.58	0.19	0.39	1.93	1.81	0.12	6.8	0.85	5.9
16	Al-Edd Al-Gharbi	46.55	641	9.2	0.06	9.2	114.2	4.69	109.53	1.00	0.01	0.99	0.68	0.17	0.51	2.40	1.61	0.79	35.5	0.75	34.8
17	Ash Shargi Oilfield	78.90	560	7.8	0.06	7.7	15.6	4.09	11.55	2.07	0.00	2.06	0.48	0.14	0.34	2.09	1.40	0.69	48.9	0.66	48.2
18	Halul Island	84.05	335	12.1	0.03	12.1	12.8	2.45	10.33	2.74	0.00	2.74	0.43	0.09	0.35	2.65	0.84	1.81	12.7	0.39	12.3
19	High North	74.55	1019	14.5	0.10	14.4	6.7	7.46	−0.78	2.27	0.01	2.26	0.70	0.26	0.44	2.61	2.55	0.06	13.1	1.20	11.9
20	Ras Laffan	11.40	418	19.4	0.04	19.4	2.8	3.06	−0.28	1.77	0.00	1.76	0.39	0.11	0.28	3.29	1.05	2.25	14.1	0.49	13.6
21	Dukhan	0.02	5560	19.5	0.55	19.0	37.6	40.69	−3.12	0.59	0.05	0.54	2.28	1.43	0.84	14.35	13.92	0.43	9.5	6.53	3.0
22	Umm Bab	0.48	1865	9.5	0.18	9.3	17.5	13.65	3.83	0.43	0.02	0.42	1.39	0.48	0.91	4.62	4.67	−0.05	8.7	2.19	6.6
	Average		1651	12.4		12.2	22.4		10.34	1.29		1.27	1.03		0.60	5.26		1.13	16.9		15.0
	2× SD		3243	9.3		9.2	63.8		66.96	1.58		1.60	1.28		0.66	8.77		2.90	26.1		27.6
	Cumulative		2262	13.9		13.7	23.4		6.88	1.32		1.30	1.13		0.55	6.86		1.20	28.7		26.0
	2× SD		5050	13.2		12.9	53.1		52.08	1.80		1.82	1.39		0.52	11.94		3.58	79.5		79.9

Table 2. Continued.

	Bulk plankton (50 µm)		Fe			Mn			Mo			Ni			Pb			V			Zn		
Sample no.	Location	Distance (km)	*R*	*L*	*E*	*R*	*L*	*E*	*R*	*L*	*E*	*R*	*L*	*E*	*R*	*L*	*E*	*R*	*L*	*E*	*R*	*L*	*E*
1	Doha	10.19	1359	1384	−24.4	26.3	26.3	−0.02	116.86	0.18	116.67	5.99	4.26	1.73	0.70	0.45	0.25	4.59	4.84	−0.25	25.5	10.5	15.0
2	Khor Al-Odaid	0.23	793	530	262.7	52.2	10.1	42.1	2.59	0.07	2.52	2.94	1.63	1.31	0.34	0.17	0.17	26.74	1.86	24.89	78.9	4.0	74.9
3	Mesaieed	0.60	2200	1608	592.1	50.1	30.5	19.5	9.26	0.21	9.04	7.71	4.95	2.76	3.01	0.52	2.49	18.70	5.63	13.08	184.5	12.2	172.3
4	Shraawoo	59.60	1023	1037	−14.0	35.5	19.7	15.8	17.58	0.14	17.44	4.77	3.19	1.58	0.50	0.34	0.16	6.62	3.63	2.99	89.8	7.9	82.0
5	Al-Edd Al-Gharbi	46.55	239	256	−17.3	13.2	4.9	8.3	0.00	0.03	−0.03	1.17	0.79	0.38	0.33	0.08	0.25	1.27	0.90	0.37	24.5	1.9	22.6
6	Ash Shargi Oilfield	78.90	977	977	0.8	31.7	18.5	13.1	0.31	0.13	0.18	5.27	3.01	2.26	0.80	0.32	0.48	5.27	3.42	1.85	68.7	7.4	61.3
7	Halul Island	84.05	437	548	−110.6	16.0	10.4	5.6	0.27	0.07	0.19	5.20	1.69	3.51	0.19	0.18	0.01	2.05	1.92	0.13	73.7	4.2	69.6
8	High North	74.55	526	631	−104.9	21.5	12.0	9.5	0.00	0.08	−0.08	4.26	1.94	2.32	0.31	0.20	0.11	1.97	2.21	−0.24	36.6	4.8	31.8
9	Ras Laffan	11.40	445	429	16.6	12.8	8.1	4.6	0.34	0.06	0.28	3.12	1.32	1.80	0.80	0.14	0.66	2.08	1.50	0.58	98.8	3.3	95.5
10	Dukhan	0.02	5493	5617	−123.2	132.7	106.7	26.1	0.18	0.75	−0.57	21.06	17.30	3.77	3.03	1.82	1.20	27.31	19.66	7.66	48.5	42.7	5.8
11	Umm Bab	0.48	3628	3857	−229.3	88.6	73.3	15.3	0.32	0.51	−0.20	14.11	11.88	2.23	2.12	1.25	0.87	19.28	13.50	5.78	41.7	29.3	12.4
	Average		1556		22.6	43.7		14.5	13.43		13.22	6.87		2.15	1.10		0.60	10.54		5.17	70.1		58.5
	2× SD		3270		450.0	74.1		23.4	69.50		69.52	11.56		1.93	2.17		1.45	20.67		15.52	91.3		98.1
	Zooplankton (200 µm)		*R*	*L*	*E*	*R*	*L*	*E*	*R*	*L*	*E*	*R*	*L*	*E*	*R*	*L*	*E*	*R*	*L*	*E*	*R*	*L*	*E*
12	Doha	10.19	1770	1736	34.2	37.2	33.0	4.2	66.15	0.23	65.92	7.30	5.35	1.96	1.15	0.56	0.58	6.50	6.08	0.42	49.2	13.2	36.0
13	Khor Al-Odaid	0.23	817	540	277.5	75.3	10.3	65.0	2.98	0.07	2.90	3.15	1.66	1.49	0.18	0.18	0.01	10.47	1.89	8.58	90.1	4.1	86.0
14	Mesaieed	0.60	2001	1480	521.0	57.1	28.1	29.0	17.63	0.20	17.44	7.57	4.56	3.01	2.03	0.48	1.55	9.69	5.18	4.51	74.6	11.2	63.3
15	Shraawoo	59.60	370	385	−15.7	27.0	7.3	19.7	17.74	0.05	17.69	1.73	1.19	0.54	0.16	0.13	0.04	2.99	1.35	1.64	42.3	2.9	39.3
16	Al-Edd Al-Gharbi	46.55	315	342	−26.9	20.3	6.5	13.8	0.00	0.05	−0.05	1.58	1.05	0.52	0.56	0.11	0.45	1.80	1.20	0.60	46.7	2.6	44.1
17	Ash Shargi Oilfield	78.90	262	299	−36.8	15.3	5.7	9.7	0.00	0.04	−0.04	1.55	0.92	0.63	0.00	0.10	−10.00	1.88	1.04	0.84	61.7	2.3	59.5
18	Halul Island	84.05	136	179	−42.4	5.7	3.4	2.3	0.10	0.02	0.08	2.03	0.55	1.48	0.14	0.06	0.08	0.91	0.62	0.28	64.9	1.4	63.6
19	High North	74.55	484	544	−59.9	22.5	10.3	12.1	0.00	0.07	−0.07	3.90	1.67	2.23	0.57	0.18	0.39	2.17	1.90	0.27	45.9	4.1	41.8
20	Ras Laffan	11.40	222	223	−1.3	7.7	4.2	3.5	0.98	0.03	0.95	2.80	0.69	2.11	0.00	0.07	−0.07	1.22	0.78	0.44	80.6	1.7	78.9
21	Dukhan	0.02	2923	2967	−44.0	79.2	56.4	22.9	0.00	0.40	−0.04	11.60	9.14	2.46	1.58	0.96	0.62	14.67	10.38	4.29	67.3	22.5	44.8
22	Umm Bab	0.48	988	996	−7.3	82.5	18.9	63.6	0.00	0.13	−0.13	3.98	3.07	0.92	0.89	0.32	0.57	5.30	3.48	1.82	41.8	7.6	34.2
	Average		935		54.4	39.1		22.3	9.60		9.48	4.29		1.58	0.66		0.37	5.24		2.15	60.5		53.8
	2× SD		1823		361.6	58.6		44.7	39.99		39.92	6.43		1.70	1.36		0.96	9.17		5.25	33.2		35.3
	Cumulative		1246		38.5	41.4		18.4	11.51		11.35	5.58		1.86	0.88		0.49	7.89		3.66	65.3		56.1
	2× SD		2661		399.6	65.3		35.8	55.47		55.44	9.50		1.87	1.82		1.22	16.52		11.72	67.8		72.1

Table 3. Data for the trace element composition of plankton from the 2014 cruise. The upper segment, data for the small-size fraction (phytoplankton), collected with a 50 µm net tow, is separated from the lower segment with data for the large-size fraction (zooplankton), collected with a 200 µm net tow. The "Cumulative" row is an average of both of these measurements. For both size classes and the Cumulative data averages and standard deviations are given. The distance column is a calculation of the shortest distance from land to each sampling location (in kilometers). The letters *R*, *L*, and *E* represent the values for raw data, the lithogenic correction (using average Qatar dust), and the excess concentrations, respectively. All concentrations are parts per million (ppm), or $\mu g\,g^{-1}$. Aluminum only has a raw data column because all of the aluminum in each sample was assumed to be of lithogenic origin, meaning that the lithogenic correction would be zero. The number in scientific notation in parentheses adjacent to the (*L*) column is a numerical representation of the [Me]/Al ratio found in average Qatari dust (Table 1 and Yigiterhan et al., 2018) used to determine the lithogenic correction. Certain elements have excess values, which are negative, indicating that there was an overcorrection for the lithogenic portion of the sample.

Bulk plankton (50 µm)			Al	As			Ba			Cd			Co			Cr			Cu		
Sample	Location	Distance (km)	*R*	*R*	*L*	*E*	*R*	*L*	*E*	*R*	*L*	*E*	*R*	*L*	*E*	*R*	*L*	*E*	*R*	*L*	*E*
23	Dukhan	8.77	4129	8.40	0.41	7.99	21.9	30.2	−8.29	0.80	0.03	0.76	1.77	1.06	0.71	10.3	10.2	0.08	36.0	4.85	31.1
24	Dukhan	6.78	4035	9.62	0.40	9.22	21.7	29.5	−7.88	0.79	0.03	0.76	1.68	1.04	0.63	8.8	10.1	−1.27	65.2	4.74	60.5
25	Dukhan	1.31	8407	14.45	0.83	13.61	42.2	61.5	−19.32	0.19	0.07	0.12	2.62	2.17	0.45	16.7	21.1	−4.32	21.7	9.87	11.8
26	Doha	6.54	4401	3.87	0.44	3.43	28.6	32.2	−3.61	0.26	0.04	0.22	1.78	1.13	0.65	15.0	11.0	3.94	311.2	5.17	306.0
27	Doha	2.20	3266	2.01	0.32	1.68	12.5	23.9	−11.37	0.09	0.03	0.06	1.41	0.84	0.57	8.9	8.2	0.69	44.8	3.84	41.0
28	Doha	0.06	14 493	4.54	1.44	3.11	69.5	106.1	−36.58	0.10	0.12	−0.02	3.86	3.74	0.12	44.0	36.3	7.70	35.9	17.02	18.9
	Average		6455	7.15		6.51	32.7		−14.51	0.37		0.32	2.19		0.52	17.3		1.14	85.8		78.2
	2× SD		8675	9.16		9.14	41.0		24.04	0.67		0.70	1.83		0.43	27.0		8.38	222.7		225.8
Zooplankton (200 µm)																					
Sample	Location	Distance (km)	*R*	*R*	*L*	*E*	*R*	*L*	*E*	*R*	*L*	*E*	*R*	*L*	*E*	*R*	*L*	*E*	*R*	*L*	*E*
29	Dukhan	8.77	2054	7.04	0.20	6.83	14.1	15.0	−0.90	0.77	0.02	0.75	2.45	0.53	1.92	−27.2	5.1	−32.36	31.9	2.41	29.5
30	Dukhan	6.78	4448	5.83	0.44	5.39	78.4	32.6	45.83	0.29	0.04	0.25	1.75	1.15	0.60	17.5	11.1	6.34	6.9	5.22	1.6
31	Dukhan	1.31	4190	5.17	0.41	4.76	33.9	30.7	3.19	0.12	0.03	0.09	2.15	1.08	1.07	12.6	10.5	2.08	124.8	4.92	119.9
32	Doha	6.54	3729	4.10	0.37	3.73	22.0	27.3	−5.28	0.62	0.03	0.59	1.79	0.96	0.82	12.7	9.3	3.39	367.6	4.38	363.3
33	Doha	2.20	7634	2.45	0.76	1.69	40.9	55.9	−14.97	0.37	0.06	0.30	4.25	1.97	2.28	44.4	19.1	25.23	28.0	8.97	19.1
34	Doha	0.06	5506	4.86	0.55	4.32	24.8	40.3	−15.49	0.33	0.05	0.28	4.34	1.42	2.92	23.7	13.8	9.88	29.5	6.47	23.0
	Average		4594	4.91		4.45	35.7		2.06	0.41		0.38	2.79		1.60	18.5		2.43	98.1		92.7
	2× SD		3737	3.12		3.44	45.8		45.42	0.47		0.49	2.39		1.83	29.8		37.98	276.7		277.9
	Cumulative		5524	6.03		5.48	34.2		−6.22	0.39		0.35	2.49		1.06	17.9		1.78	92.0		85.5
	2× SD		6659	6.93		6.92	41.6		42.18	0.55		0.58	2.12		1.70	27.1		26.26	239.8		241.9

Table 3. Continued.

Bulk plankton (50 µm)			Fe			Mn			Mo			Ni			Pb			V			Zn		
Sample	Location	Dist. (km)	*R*	*L*	*E*	*R*	*L*	*E*	*R*	*L*	*E*	*R*	*L*	*E*	*R*	*L*	*E*	*R*	*L*	*E*	*R*	*L*	*E*
23	Dukhan	8.77	2358	2204	155	44.1	41.85	2.3	0.29	0.29	0.002	9.7	6.79	2.9	1.3	0.72	0.6	17.0	7.71	9.3	116	16.74	99
24	Dukhan	6.78	2305	2111	194	43.1	40.90	2.2	0.14	0.29	−15.00	9.2	6.63	2.6	3.4	0.70	2.7	16.7	7.54	9.2	77	16.35	60
25	Dukhan	1.31	4258	4486	−228	68.5	85.21	−16.8	0.10	0.59	−0.49	15.5	13.82	1.7	2.7	1.46	1.3	21.2	15.70	5.5	30	34.07	−4
26	Doha	6.54	2603	2349	255	40.1	44.60	−4.5	0.48	0.31	0.17	9.7	7.23	2.4		0.76		11.1	8.22	2.9	147	17.84	129
27	Doha	2.20	1752	1743	9	23.4	33.11	−9.7	−0.19	0.23	−0.43	6.5	5.37	1.1	2.2	0.57	1.7	8.3	6.10	2.2	45	13.24	32
28	Doha	0.06	7205	7735	−530	150.2	146.90	3.3	0.40	1.03	−0.63	19.8	23.82	−4.0	6.2	2.51	3.7	48.4	27.07	21.3	67	58.75	9
	Average		3414		−24	61.6		−3.9	0.20		−0.25	11.7		1.1	3.2		2.0	20.4		8.4	80		54
	2× SD		4084		604	91.5		16.2	0.49		0.62	9.8		5.2	3.7		2.4	28.9		14.0	88		104
Zooplankton (200 µm)																							
Sample	Location	Dist. (km)	*R*	*L*	*E*	*R*	*L*	*E*	*R*	*L*	*E*	*R*	*L*	*E*	*R*	*L*	*E*	*R*	*L*	*E*	*R*	*L*	*E*
29	Dukhan	8.77	1757	1096	661	45.8	20.82	25.0	−1.67	0.15	−1.82	20.9	3.38	17.5	1.1	0.36	0.6	16.8	3.84	13.0	60	8.33	52
30	Dukhan	6.78	3275	2374	902	83.4	45.08	38.3	−1.78	0.32	−2.10	16.9	7.31	9.6	−0.7	0.77	−1.8	49.9	8.31	41.6	35	18.03	17
31	Dukhan	1.31	3299	2236	1063	70.3	42.46	27.8	−1.33	0.30	−1.63	14.1	6.89	7.2	26.7	0.73	25.7	14.9	7.82	7.1	140	16.98	123
32	Doha	6.54	2874	1990	884	45.6	37.80	7.8	−0.80	0.27	−1.06	17.2	6.13	11.1		0.65		13.5	6.96	6.5	472	15.12	457
33	Doha	2.20	5932	4074	1858	184.4	77.38	107.0	−0.11	0.54	−0.07	24.3	12.55	11.7	128.8	1.32	126.9	32.9	14.26	18.6	134	30.94	103
34	Doha	0.06	3434	2939	495	482.5	55.81	426.6	0.57	0.39	0.18	14.9	9.05	5.8	152.9	0.95	151.6	26.0	10.28	15.7	380	22.32	357
	Average		3429		977	152.0		105.4	0.10		−1.18	18.0		10.5	61.9		60.6	25.7		17.1	204		185
	2× SD		2,743		951	339.7		322.1	0.46		0.15	7.7		8.2	146.7		146.2	28.0		25.8	359		358
	Cumulative		3421		452	106.8		50.8	0.15		−0.72	14.9		5.8	32.5		31.3	23.1		12.7	142		120
	2× SD		3317		1292	255.3		245.6	0.47		1.56	10.7		11.8	115.8		115.4	27.7		21.8	280		286

Qatari dust (from Table 1). The excess concentrations calculated that way were often negative because the "apparent" lithogenic correction was so much larger. As these values are unrealistic, those calculations are shown in Tables S1 (2012) and S2 (2014) in the Supplement.

The differences between the average excess metal concentrations in small (50 µm) and large (200 µm) net-tow samples are shown in Fig. 4. The average compositions of the two size classes were in good agreement when you consider the standard deviations. We ran t tests to determine whether the average small and large plankton samples were statistically different. For the 2012 data, there were only small statistical differences for Ni and V. For the 2014 data, there were small statistical differences for Cr, Cu, Fe, and Ni. Thus, we combined the data sets (50 + 200 µm) and reported the grand average and standard deviation for all samples as the cumulative rows at the bottom of Tables 2 and 3.

We conducted statistical tests to determine whether the cumulative means of the excess concentrations (E) in Tables 2 and 3 were different from zero. If column E were not statistically different from zero, it would support the argument that the elemental concentrations in the particulate samples were totally due to the presence of lithogenic material (Qatari dust) and the contributions from plankton and anthropogenic sources were insignificant. The outcomes of the statistical evaluations are shown in Table 4 (for 2012 data) and Table 5 (for 2014 data).

All tests to determine whether E was different from zero were one-sample tests using the combined plankton for a given year. They were also one-sided with the alternative hypothesis that the sample was greater than zero. To decide which test to use, we first had to use the Shapiro test to establish whether the sample concentrations were normally distributed. If the Shapiro test is greater than 0.05, distributions are normal. The outcomes regarding normality are listed in the fifth column. Most distributions are not normal. If distributions are normal, you can use the t test. If not normal, you have to use the Wilcoxon rank test. The sixth column shows the test used. For the 2012 sample set, only Ni was normally distributed (Table 4). For 2014 As, Cd, Fe, and Ni were normal (Table 5).

We used the Wilcoxon rank test with alpha = 0.5 and the output is a p value for the difference of the median from zero. Those p values are shown in the third column. The answer to the question "Is the value of column E different from zero?" is given in the second column (Tables 4, 5).

4 Discussion

Most marine particulate matter is composed of material of biotic origin with minor contributions from atmospheric dust (Ho et al., 2007; Rauschenberg and Twining, 2015). The Qatari EEZ is an especially unique site to study marine particulate matter because of the large deposition rates of atmospheric dust. After marine particulate matter is corrected for the contribution of dust, we look for an answer to the question "Can plankton and anthropogenic signals still be identified in the remaining concentrations?".

4.1 Regional dust composition

The transport and deposition of aeolian dust are widely recognized as an important physical and chemical concern to climate, human health, and marine ecosystems (Rashki et al., 2013). Qatar is in a region heavily affected by dust storms originating from a multitude of sources. Back trajectories show that winds come from a variety of locations, but mostly either from the northwest (northern Saudi Arabia and Iraq) or the southeast (Oman) (Yigiterhan et al., 2018). Because dust is potentially such an important source of lithogenic particles to the surface waters of the central part of the Arabian Gulf, determining the composition of the total and potentially soluble dust end-member concentrations was an important part of this study. Ideally, with well-established end-members, we could analyze the composition of the size-fractionated particulate matter and determine the relative contributions of the dust and plankton end-members and possible anthropogenic contributions. Fortunately, in this study, the composition of local dust in Qatar has been well characterized. This dust is carbonate rich, which is different from the composition of atmospheric dust from most other regions around the world, which is dominated by aluminosilicate material (e.g., Prospero et al., 1981; Mahowald et al., 2005; Lawrence and Neff, 2009; Muhs et al., 2014; Patey et al., 2015).

The concentrations of all major and trace elements in Qatari dust are different from those in the average UCC (Table 1). The most notable differences between the two are the depletion of aluminum and the enrichment of calcium in Qatari dust. Yigiterhan et al. (2018) showed that the average composition of Qatari dust has concentrations of Ca much higher than those predicted by the crustal Ca/Al ratios, suggesting that $CaCO_3$(s), and possibly $CaSO_4$(s) minerals, are a major component of the total mass. In the UCC, aluminum has a higher concentration (8.2 %) than calcium (2.6 %). However, in unleached Qatari dust, the two elements switch positions, with aluminum decreasing to 2.1 % by weight versus calcium, which is elevated to 13.7 % by weight (Table 1). Qatari dust has over 5.3 times the amount of calcium and about a quarter of the amount of aluminum compared to the UCC. By converting Ca to $CaCO_3$ and comparing it with the total mass, we calculate that carbonate minerals make up 35 % or more of the total mass. The reason for this is due to the abundance of carbonate minerals in rock outcrops and soils in the Qatar Peninsula, thereby allowing carbonate minerals (calcite and dolomite) to be a major component of dust via erosional processes. The majority of the Qatar Peninsula is underlain by uniform limestone beds of Miocene and Eocene age (Sadooni et al., 2014), and the source areas to the north and south are similar. As a result,

Table 4. Are dust-corrected plankton concentrations statistically different from zero for 2012 data?

Element	> Zero	p_value	Shapiro	not_normal	test_used	t_test	Wilcoxon
As	Yes	0.000	0.007	non_normal	Wilcoxon	0.000	0.000
Ba	No	0.538	0.000	non_normal	Wilcoxon	0.114	0.538
Cd	Yes	0.000	0.013	non_normal	Wilcoxon	0.000	0.000
Co	Yes	0.000	0.005	non_normal	Wilcoxon	0.000	0.000
Cr	Yes	0.001	0.007	non_normal	Wilcoxon	0.002	0.001
Cu	Yes	0.000	0.000	non_normal	Wilcoxon	0.003	0.000
Fe	No	0.815	0.000	non_normal	Wilcoxon	0.188	0.815
Mn	Yes	0.000	0.001	non_normal	Wilcoxon	0.000	0.000
Mo	Yes	0.009	0.000	non_normal	Wilcoxon	0.034	0.009
Ni	Yes	0.000	0.637	normal	*t* test	0.000	0.000
Pb	Yes	0.001	0.000	non_normal	Wilcoxon	0.469	0.001
V	Yes	0.000	0.000	non_normal	Wilcoxon	0.004	0.000
Zn	Yes	0.000	0.019	non_normal	Wilcoxon	0.000	0.000

Table 5. Are dust-corrected plankton concentrations statistically different from zero for 2014 data?

Element	> zero	p_value	Shapiro	not_normal	test_used	t_test	Wilcoxon
As	Yes	0.000	0.156	normal	*t* test	0.000	–
Ba	No	0.979	0.019	non_normal	Wilcoxon	–	0.979
Cd	Yes	0.001	0.059	normal	*t* test	0.001	–
Co	Yes	0.000	0.017	non_normal	Wilcoxon	–	0.000
Cr	No	0.102	0.022	non_normal	Wilcoxon	–	0.102
Cu	Yes	0.000	0.000	non_normal	Wilcoxon	–	0.000
Fe	Yes	0.013	0.923	normal	*t* test	0.013	–
Mn	Yes	0.046	0.000	non_normal	Wilcoxon	–	0.046
Mo	No	0.995	0.000	non_normal	Wilcoxon	–	0.995
Ni	Yes	0.003	0.817	normal	*t* test	0.003	–
Pb	Yes	0.012	0.000	non_normal	Wilcoxon	–	0.012
V	Yes	0.000	0.017	non_normal	Wilcoxon	–	0.000
Zn	Yes	0.000	0.004	non_normal	Wilcoxon	–	0.000

the composition of Qatari dust from the northern and southern regions is very similar for most elements (Yigiterhan et al., 2018).

The enrichment of calcium carbonate, along with other possible metal–$CaCO_3$ associations, leads to uncertainty regarding how to best use the dust samples for the lithogenic correction. Because calcium carbonate is more soluble than aluminosilicates, samples leached with HAc–HyHCl may in fact be a more accurate representation of the actual concentration to use for the lithogenic correction. The compositions of Qatari dust before and after the leaching process are compared in Table 1. Because the emphasis of the study was on particles, we focused on how the composition of the particles changes rather than on how much of the different elements was solubilized. Certain elements that are usually associated with calcium carbonates (e.g., Mg, Sr, Li) are elevated relative to the UCC in dust samples prior to leaching. If elements associated with these carbonate minerals are solubilized in seawater, our results show that their concentrations in the leached dust samples could be elevated relative to aluminum, causing the Me/Al ratio to be elevated as well. You would normally expect that this leach would remove and lower the concentrations of reactive elements. However, all elements other than Ca and Li increased in concentration because the mass removed by the leach was more important than the removal of the individual elements by the leach. As a result of mass removal during the leach, the concentrations of Mo (3350 %), Ni (511 %), As (234 %), Ba (204 %), Cr (179 %), Pb (148 %), Zn (149 %), Fe (132 %), K (111 %), and Al (105 %) in the leached solids more than doubled. The difference between total and leached Qatari dust samples expressed as the percent difference from the total composition is shown as a bar graph in Fig. 3.

4.2 Fate of dust in seawater

It is uncertain how the composition of Qatari dust might be modified when the particles enter surface seawater. Do the particles keep the composition they had in the atmosphere or does the $CaCO_3$ dissolve (completely or partially),

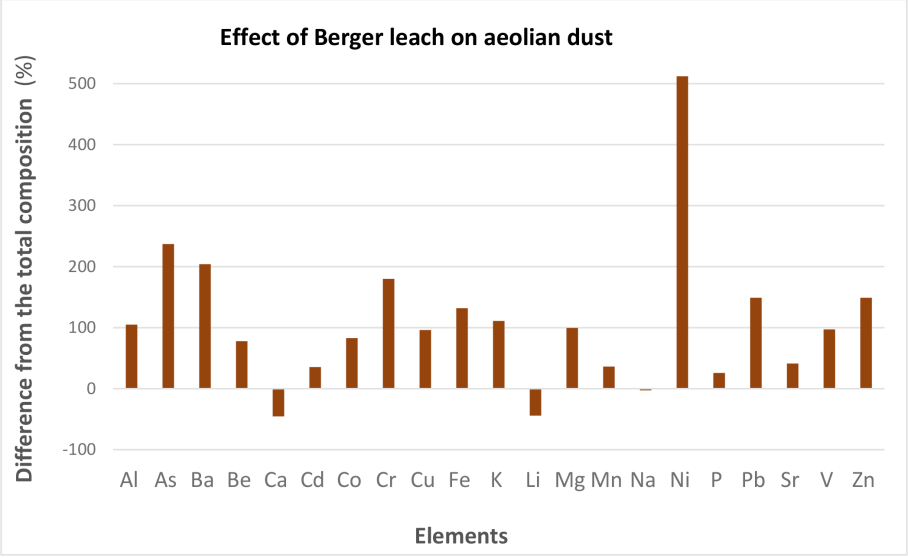

Figure 3. The difference between unleached and leached Qatari dust samples expressed as the percent difference from the unleached composition. Molybdenum (Mo) is not shown because its difference (+3350 %) was off scale.

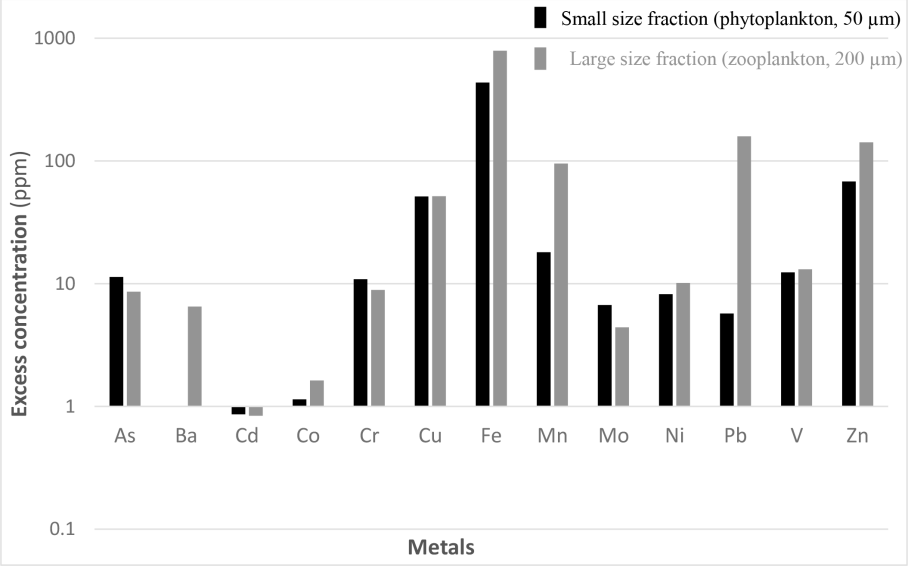

Figure 4. The difference between the excess metal concentrations in the small-size fraction (50 µm, phytoplankton) and large-size fraction (200 µm, zooplankton) data sets. These represent the average of the cumulative data in the two data sets for 2012 and 2014. The vertical axis is logarithmic. The value for Ba in the phytoplankton data is not shown because it was negative due to overcorrection and could not be plotted on a logarithmic graph.

thus changing the Me/Al ratios of the residual material? Carbonate mineral dissolution would be driven by the saturation state in the water column. Very little is known about the carbonate chemistry in the Arabian Gulf, though a limited early study in 1977 (Brewer and Dyrssen, 1985) suggested that the surface seawaters were saturated with respect to calcite and that $CaCO_3$ is being formed. One possible benefit of this carbonate-rich dust might be to buffer future increases in ocean acidification (Doney et al., 2009) in the Arabian Gulf.

As a result of this weak acid leach much of the carbonate mineral (and associated element) fraction in Qatari dust was removed into leachate solution. Equating the conditions of the Berger et al. (2008) leach with what happens to dust particles upon deposition in seawater is highly problematic. However, the leached dust gives the most extreme outcome where most of the $CaCO_3$(s) and associated elements were solubilized and removed. The elements that have net removal by the leach have a ratio < 1 and include Ca and Li. The

concentrations of all other elements increased in the leached material because of the reduction of mass. The ratio for Na was close to 1.0 (0.97), which suggests that our sample rinse procedure after collection removed most of the sea salt contamination. The data in Table 1 show that after the leach Ca decreased by 45 % and Li by 44 %.

We have recently found high concentrations of particulate Ca in a new set of particulate net-tow samples (Yigiterhan et al., unpublished data, 2020). Significant Ca (> 95 %) is removed from both size fractions by the HAc–HyHCl leach, suggesting that $CaCO_3$(s) is present in those water column particulate matter samples. $CaCO_3$-forming plankton are rare in the Arabian Gulf (Quigg et al., 2013; Polikarpov et al., 2016). Thus, these data suggest that $CaCO_3$ in Qatari dust does not dissolve upon entering seawater after atmospheric deposition. This justifies our use of the unleached dust concentrations for the lithogenic correction.

4.3 How much of the trace element composition is controlled by dust?

Atmospheric dust makes a major contribution to particles in the water column of the Arabian Gulf. After making the lithogenic correction, we found that some elements had no excess concentrations that could be attributed to plankton or anthropogenic sources. For the year 2012, two elements (Ba and Fe) were not statistically different from zero. This means that the input of Qatari dust can explain the Ba and Fe composition in Qatari marine particulate matter. The rest were different from zero and there is a statistically recognizable biological/anthropogenic component. For the year 2014, Ba, Cr, and Mo were not statistically different from zero. Traditional box plots showing these differences visually are shown in Fig. 5.

4.4 Metal to aluminum ratios

Another approach for examining the question regarding the importance of input from Qatari dust and excess metal concentrations is to use plots of metal versus aluminum concentrations (Fig. 6). We argue that those elements that correlate strongly with Al and have the same metal to aluminum (Me/Al) ratio as dust may be controlled by dust input. The Me/Al plots include a best fit linear regression (solid line) and lines representing the Me/Al in the average UCC (long dashes) (Rudnick and Gao, 2003) and average Qatari dust (short dashes) (Table 1).

The grouping of elements is pretty clear. The elements with trends parallel to Qatari dust include Co, Cr, Fe, Mn, Ni, Pb, and Li. Vanadium increases with Al but at a higher rate. This may be due to scavenging of V from seawater, as proposed by Jeandel et al. (1987) for the Mediterranean. Barium increases with Al but at a lower rate. Perhaps Ba can be solubilized out of the dust when it enters seawater. Molybdenum mostly increases with Al in agreement with Qatari dust with the exception of six samples, from the year 2012 data set, at low Al that have large excess Mo. Arsenic and Cu are uniformly higher than expected for Qatari dust and Cd is higher, especially at low Al concentrations. It is tempting to speculate that these elements are higher due to biological enrichment. Metal to phosphorus (Me/P) ratios are required for comparison with other studies of plankton composition. But in the absence of data for P, we cannot separate plankton from anthropogenic sources in this study.

Table 6. Percent of total concentration that is represented by E (the difference between total minus dust contribution). The larger the contribution from dust, the lower the percentage.

Element	% E (2012)	% E (2014)
Al	0	0
As	98	91
Ba	29	−28
Cd	98	87
Co	48	40
Cr	17	11
Cu	90	90
Fe	3	9
Mn	44	49
Mo	99	$-X$
Ni	33	31
Pb	55	98
V	46	52
Zn	85	82

4.5 Plankton and anthropogenic sources

In addition to Qatari dust, plankton and anthropogenic sources are likely contributors to particle chemistry. For those elements where the average and standard deviations for the cumulative average particulate samples are not significantly different from zero, this means we cannot identify the plankton composition by difference. That was the case for Ba and Fe in the 2012 samples and for Ba, Cr, and Mo in the 2014 data set. This is an oligotrophic region with typical chlorophyll concentrations of 0.3–1.5 $\mu g\,L^{-1}$ (e.g., Al-Ansari et al., 2015). It appears that plankton are just not abundant enough relative to the input of dust to be detected by the uncertainties in this approach.

For each element, we calculated the percent of the total concentration that was represented by the difference of the total minus dust (E). The percentages are given in Table 6. Based on the combination of the statistical analysis and the plots of Me versus Al, we propose the following generalizations. These are proposed here as hypotheses that can be tested with future data sets that include Ca and P analyses. Our tentative generalizations are that

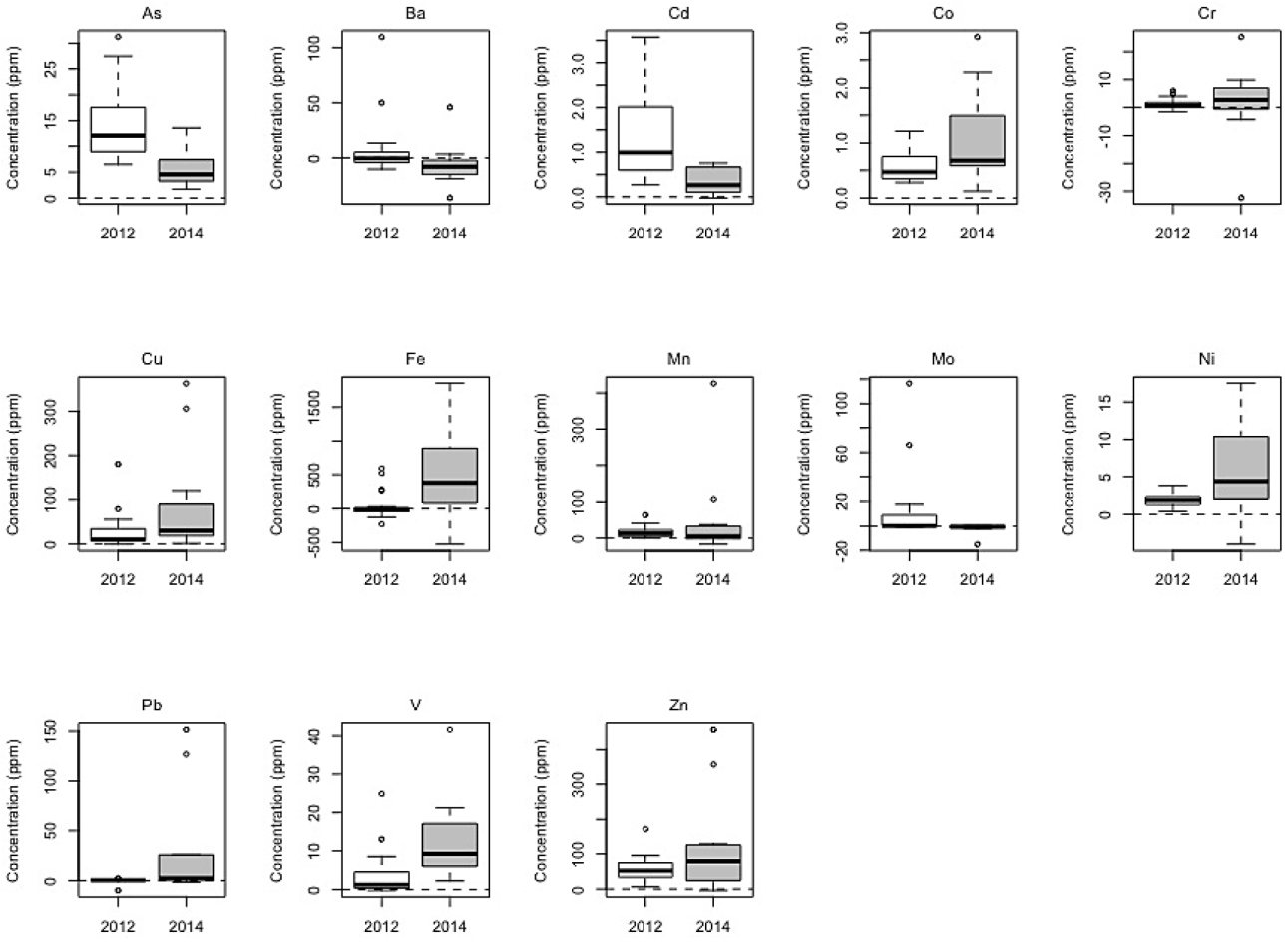

Figure 5. Box plots for statistical texts. Traditional box plot where the whiskers extend to 1.5 times in the interquartile range and then any points that fall outside of that are shown as individual dots on the graph. The dashed line at zero serves as an indicator of where the distribution lies relative to zero.

1. some elements in net-tow plankton samples could be mostly of lithogenic (dust) origin ($E < 50\,\%$ of the total). These include Al, Fe, Cr, Co, Mn, Ni, Pb, and Li.

2. Some elements may be mostly of biogenic/anthropogenic origin ($E > 80\,\%$ of the total).

   These include As, Cd, Cu, Mo, and Zn.

4.6 Regional trends

The excess metal concentrations are what originate from plankton and anthropogenic sources. In order to examine regional variability, we plotted the excess metal concentrations from Tables 2 and 3 versus distance from the shore (Fig. 7). Best-fit linear regressions are included to represent trendlines. Excess concentrations for most elements decreased with distance from the shore (Fig. 7). Ten of the 13 elements (As, Co, Cr, Cu, Fe, Mn, Mo, Ni, Pb, V, and Zn) had high concentrations in the 0–10 km range. Several elements may also show a decreasing trend with distance greater than 10 km (Co, Cu, Fe, Mn, Ni, Pb), but the statistics are poor. Cadmium was the only element for which there was a significant increasing trend with distance, with an r^2 value of 0.68. As there was no increase in chlorophyll in the 0–10 km range it is unlikely that the high excess metal concentrations were due to biological processes. Future studies should examine this more closely.

We hypothesize that abiological coastal processes are the most likely cause of these gradients, but the exact nature of the processes is unclear. As a country heavily affected by rapid population growth and new construction, nearshore sampling sites could be influenced by pollutants from disposal from outfalls (surface and groundwater) or industrialization. Nearshore dredging and reclamation are also important processes used to recontour the coastline of Qatar and to obtain $CaCO_3$ and silicate minerals for cement factories. It is unlikely that these high values are due to dust deposition as the excess concentrations are calculated relative to average Qatari dust. This nearshore enrichment phenomenon empha-

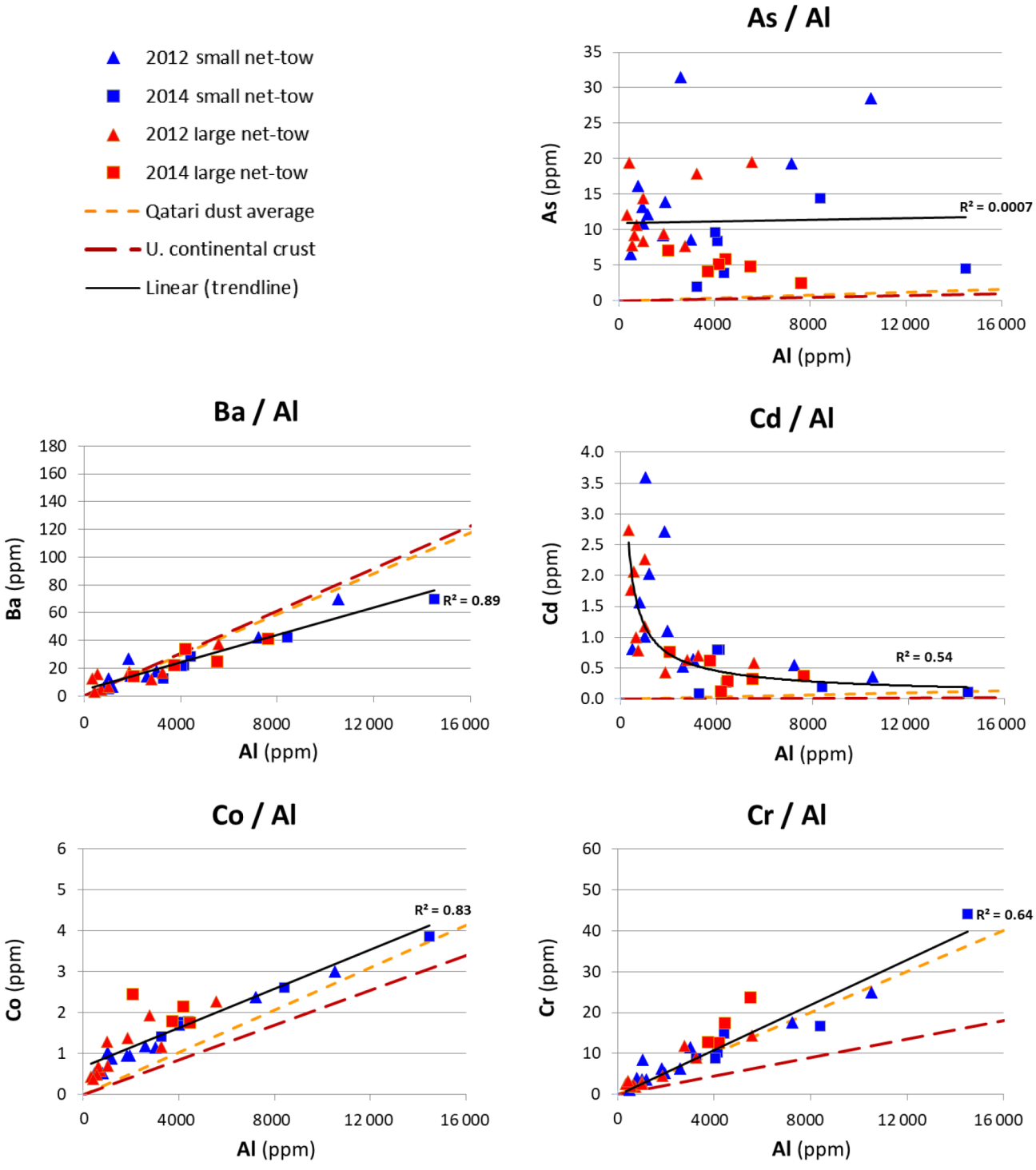
2012 small net-tow
2014 small net-tow
2012 large net-tow
2014 large net-tow
Qatari dust average
U. continental crust
Linear (trendline)
As / Al
As (ppm)
Al (ppm)
R² = 0.0007
Ba / Al
Ba (ppm)
Al (ppm)
R² = 0.89
Cd / Al
Cd (ppm)
Al (ppm)
R² = 0.54
Co / Al
Co (ppm)
Al (ppm)
R² = 0.83
Cr / Al
Cr (ppm)
Al (ppm)
R² = 0.64

Figure 6.

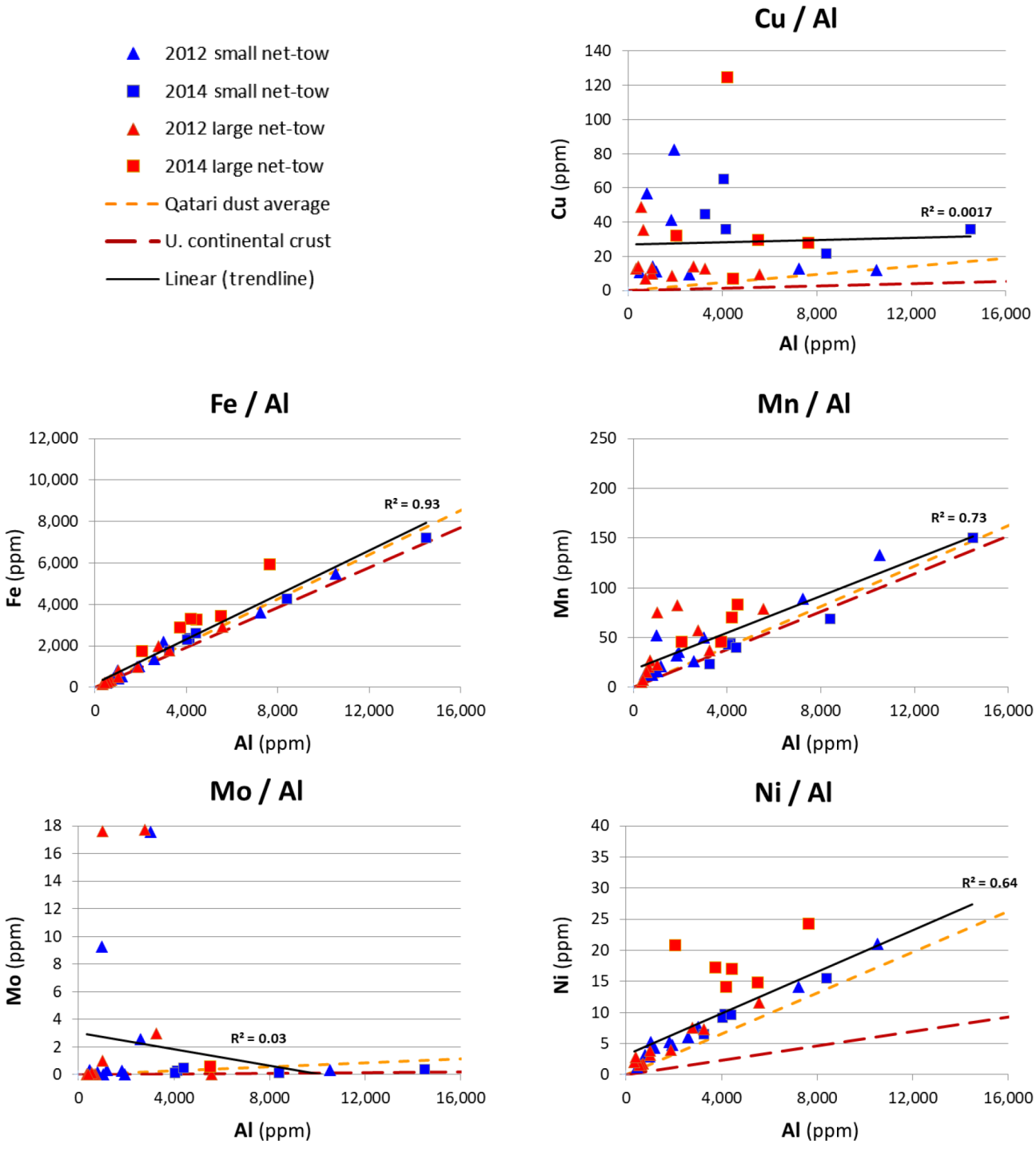
2012 small net-tow
2014 small net-tow
2012 large net-tow
2014 large net-tow
Qatari dust average
U. continental crust
Linear (trendline)
Cu / Al
Cu (ppm)
Al (ppm)
R² = 0.0017
Fe / Al
Fe (ppm)
Al (ppm)
R² = 0.93
Mn / Al
Mn (ppm)
Al (ppm)
R² = 0.73
Mo / Al
Mo (ppm)
Al (ppm)
R² = 0.03
Ni / Al
Ni (ppm)
Al (ppm)
R² = 0.64

Figure 6.

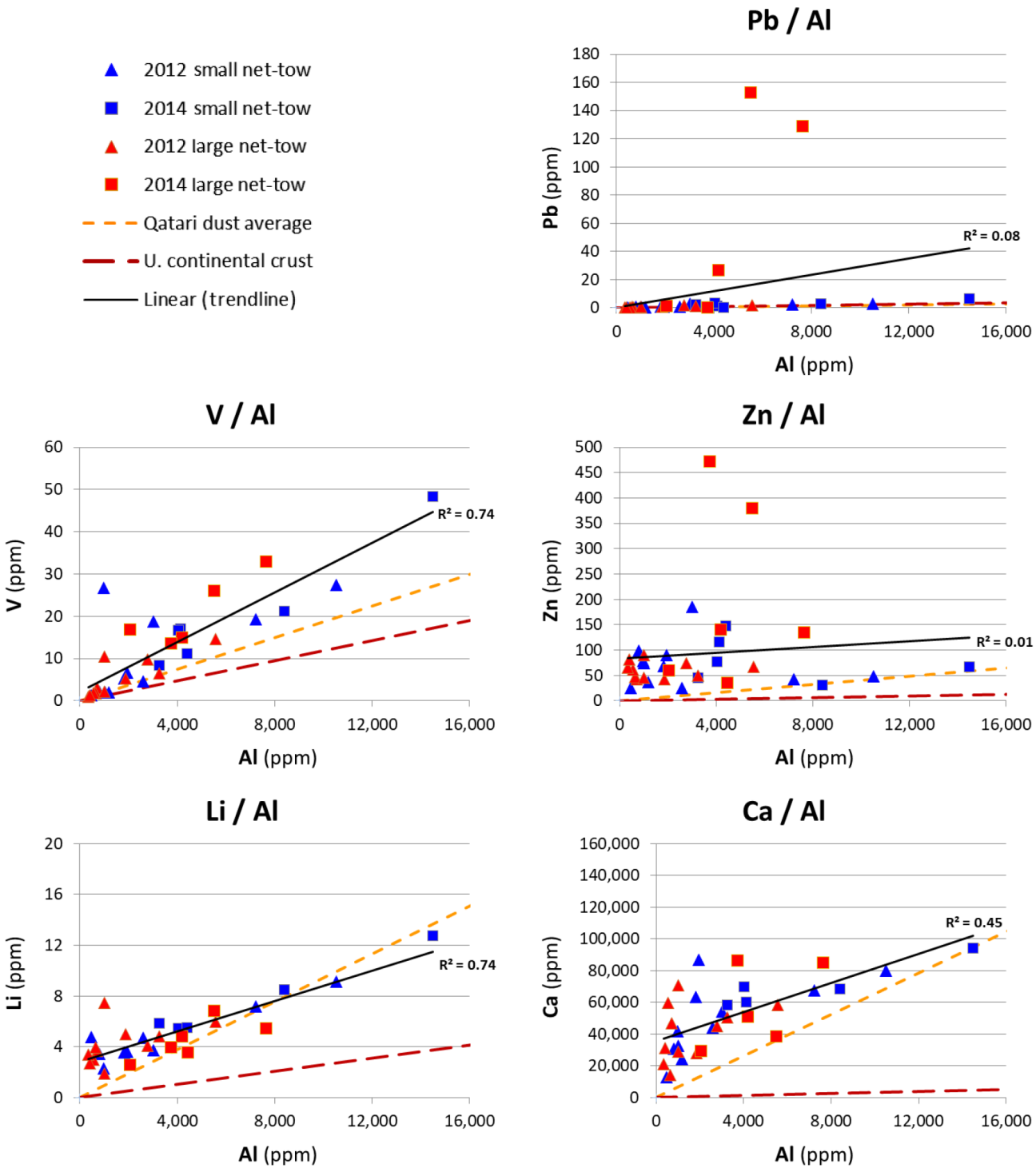

Figure 6. Metal/Al ratios for the 2012 and 2014 net-tow samples. The dashed lines represent the Me/Al in average Qatari dust (Yigiterhan et al., 2018) and Upper Continental Crust (Rudnick and Gao, 2003) values. The solid lines represent to best-fit lines for cumulative values of plankton samples. All concentrations are given in ppm.

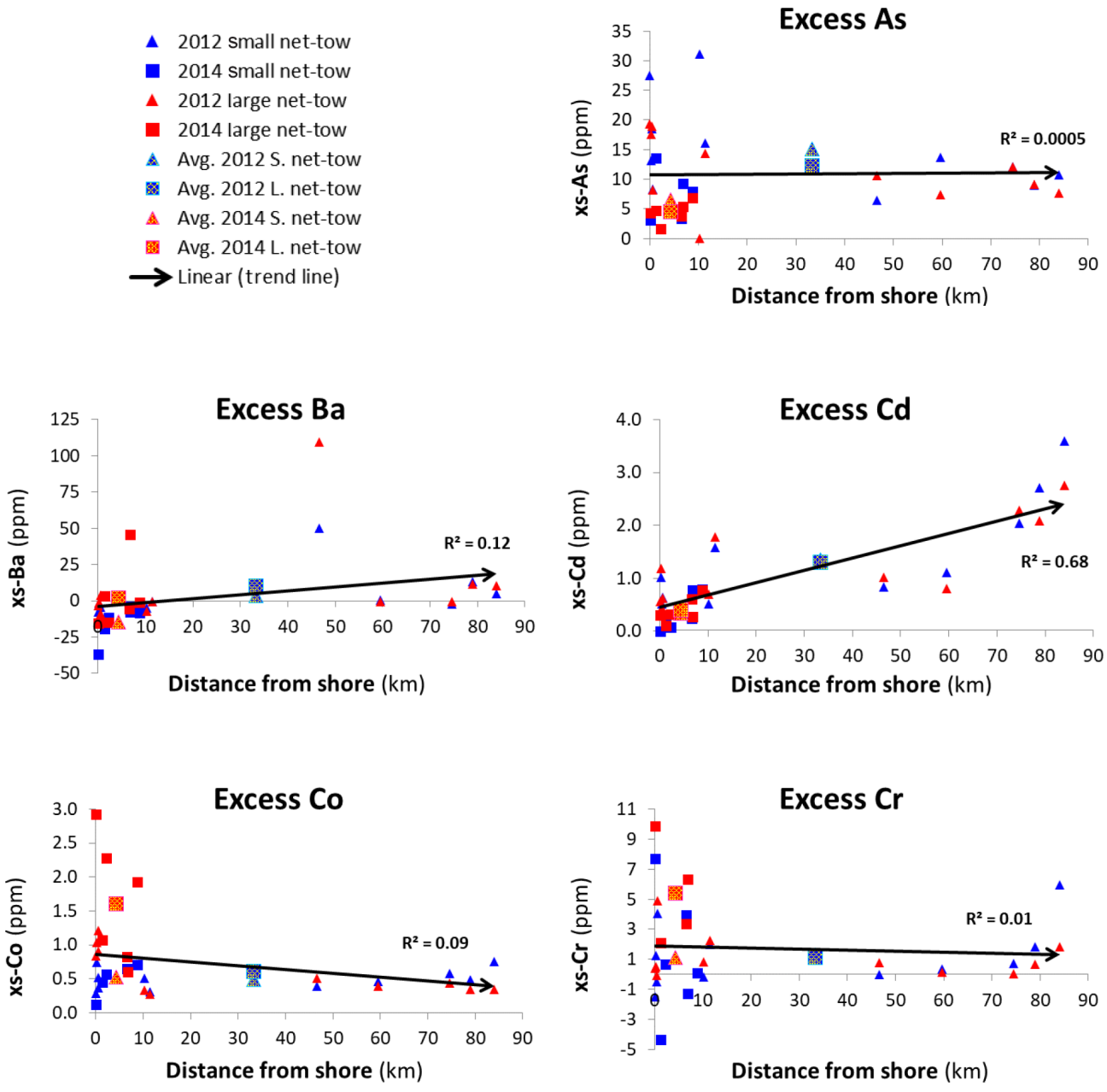

Figure 7.

sizes the need for more detailed sampling of plankton and anthropogenic sources in regions close to the shore.

5 Conclusions

Net-tow samples of natural assemblages of plankton from the Exclusive Economic Zone of Qatar in the Arabian Gulf were analyzed for elemental composition. Samples were collected using net tows with mesh sizes of 50 and 200 µm to examine size-fractionated plankton populations. Samples were collected in two different years (2012 and 2014) to examine temporal variability. Atmospheric dust from Qatar is the main source of lithogenic particles to surface seawater. Qatari dust is depleted in aluminum and enriched in calcium relative to the global average Upper Continental Crust (UCC) values. The fate of the carbonate fraction when dust particles enter seawater is uncertain; thus, we leached a subset of dust and plankton samples with an acetic acid–hydroxylamine hydrochloride procedure to solubilize $CaCO_3$ minerals and associated elements. We found that a significant amount of the Ca was solubilized but that the metal/Al ratios for many elements increased after leaching because the change in mass

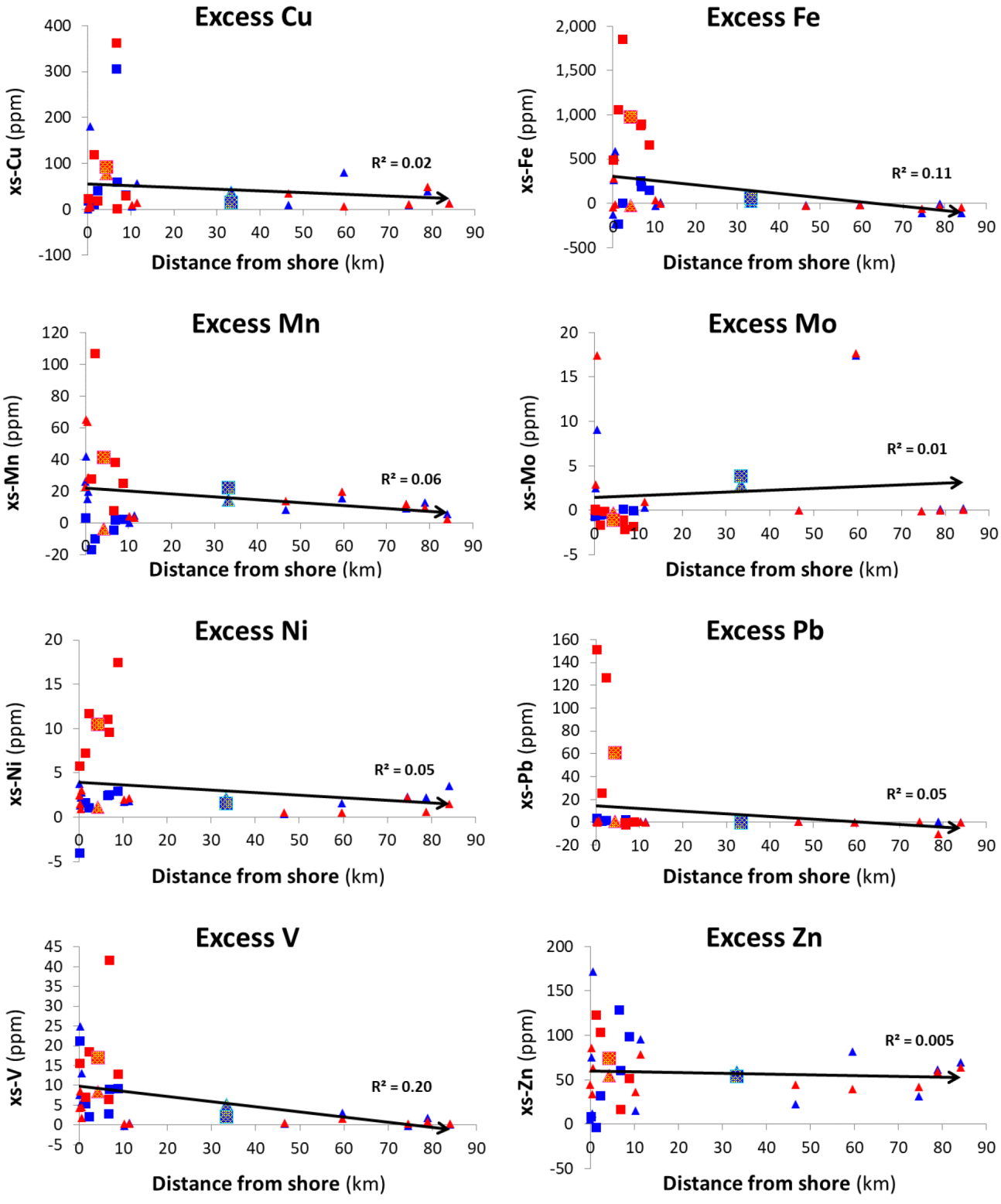

Figure 7. The excess concentrations of each element in alphabetical order after lithogenic correction using average Qatari dust versus the shortest distance from the sampling site to land. The graphs show the combined data from four data sets: 50 and 200 µm mesh net tows for both 2012 and 2014.

due to removal of $CaCO_3$ was more important than the loss of metals solubilized by the leach itself. Because the surface seawater of the Arabian Gulf appears to be supersaturated with respect to $CaCO_3$ and the concentrations of particulate Ca are large, we assumed that the $CaCO_3$ in dust does not dissolved on entering the seawater.

Excess elemental concentrations due to plankton and anthropogenic inputs were obtained by correcting total concentrations for input of atmospheric dust. Statistical analysis showed that for some elements the excess concentrations were indistinguishable from zero. This included Ba and Fe in 2012 and Ba, Cr, and Mo in 2014. This suggests that the concentrations of these elements in particulate matter can be explained as having only a dust origin. For a second approach we examined how the Me/Al ratios compared with the ratios in average Qatari dust. The elements with trends parallel to Qatari dust included Co, Cr, Fe, Mn, Ni, Pb, and Li. Vanadium increases with Al, but at a higher rate. We made tentative generalizations based on the statistical and geochemical approaches, based on the Me/Al ratios. Analysis of the net-tow plankton samples shows that there can be two major sources for these elements.

- The first group could be mostly of lithogenic (dust) origin, when excess (E) value is less than 50 % of the total concentration. These elements include Al, Fe, Cr, Co, Mn, Ni, Pb, and Li.
- The second group is of mostly biogenic or anthropogenic origin, when excess (E) value is greater than 80 % of the total concentration. These elements include As, Cd, Cu, Mo, and Zn.

The excess concentrations relative to average Qatari dust for most elements were higher in the 0 to 10 km distance from the shore. Cadmium was the one exception and had a statistically significant increase with distance from the shore. This variability could be due to differences in biology and/or nonbiological (possibly anthropogenic) processes.

Data availability. The data set underlying this paper is available at https://doi.org/10.17882/71591 (Yigiterhan et al., 2020).

Supplement. The supplement related to this article is available online at: https://doi.org/10.5194/bg-17-381-2020-supplement.

Author contributions. OY was the first and corresponding author, was NPRP Project PI, contributed to dust and plankton sampling (all campaigns), did data processing for figures and tables, and made a major contribution to the NPRP project and manuscript text writing (Material and methods; Results; Discussion), Tables 1, 2, and 3, and Figs. 1, 2, 6, and 7.

EMAA was NPRP Project PI, the sampling cruises' Chief Scientist and organizer, and coordinator of the NPRP project sampling campaigns, and provided major technical and logistic support for every step of NPRP project.

AN did the 2014 plankton sampling, lab processing and acid digestion, and text writing (Introduction).

MAAM was an NPRP Project participant, contributed to the manuscript text editing, provided passive dust samplers, and obtained the required permissions for dust sampling.

JT was responsible for Tables 1 and S1 and S2 in the Supplement, for building Figs. 3 and 4, and for data processing for leached concentrations.

HAA was responsible for all sample digestion and ICP-OES analysis for plankton and dust samples, as well as raw data processing, quality assurance, and quality control.

BP built Table 6 and Fig. 5, was a cruise participant during the 2014 plankton sampling campaigns, did lab work for cruise preparation and after cruise sample handling, filtration, and sample acid digestion, and performed data processing for calculations of excess concentrations. All leaching experiments were done by UW group members under her leadership.

IAAM was NPRP Project Co-PI and provided plankton sampling, sample gear, the research cruise sampling strategy, and logistic support, in addition to designing the experiments and contributing to plankton sampling.

MAAAAY was NPRP Project Lead-PI. MAAAAY took on the role of official leader of the project. He worked to get the required coast guard permissions, provided speedboats, and joined sampling campaigns, and helped in writing the project and some text in the manuscript.

JWM was NPRP Project Co Lead-PI and made a major contribution to the manuscript text writing (all sections), editing, and building of Tables 4 and 5. JWM also made a great contribution to this research by being team leader of the UW research team.

Competing interests. The authors declare that they have no conflict of interest.

Disclaimer. The manuscript's contents are solely the responsibility of the authors and do not necessarily represent the official views of the Qatar National Research Fund.

Acknowledgements. The authors would like to thank the Qatar National Research Fund (QNRF) for funding and supporting this research project. The dedicated effort made by the captain and crew of Qatar University R/V *Janan* during sampling was greatly appreciated. The technical help and support of Caesar Flonasca Sorino, Marwa Mustufa Al-Azhari, Azenith Castillo, Abdul Rahman Al-Obaidly, Reyniel M. Gasang, Faisal Muthar Al-Quaiti, Shafeeq Hamza, Cherriath A. Cheriath, and Mehmet Demirel from QU-ESC, during sampling, preparation, pretreatment, and analysis, are acknowledged. Colton Miller (School of Environmental and Forest Sciences, University of Washington) helped with the statistical analysis. We would like to thank Jassem Abdulaziz Al-Thani for his valuable comments and edits. We highly appreciate Qatar University, Environmental Sciences Center, Ministry of Municipality and Environment, and University of Washington-School of Oceanography administration and staff for

supporting this project at various stages. This study was made possible by a grant from the QNRF under the National Priorities Research Program.

Financial support. This research has been supported by the Qatar National Research Fund (grant no. NPRP 6-1457-1-272).

Review statement. This paper was edited by S. Wajih A. Naqvi and reviewed by two anonymous referees.

References

Al-Ansari, E. M. A. S., Rowe, G., Abdel-Moati, M. A. R., Yigiterhan, O., Al-Maslamani, I., Al-Yafei, M. A., Al-Shaikh, I., and Upstill-Goddard, R.: Hypoxia in the central Arabian Gulf exclusive economic zone (EEZ) of Qatar during summer season, Estuar. Coast. Shelf S., 159, 60–68, https://doi.org/10.1016/j.ecss.2015.03.022, 2015.

Alfoldy, B., Mahfouz, M. M. K., Yigiterhan, O., Safi, M. A., Elnaiem, A. E., and Giamberini, S.: BTEX, nitrogen oxides, ammonia and ozone concentrations at traffic influenced and background urban sites in an arid environment, Atmos. Pollut. Res., 10, 445–454, https://doi.org/10.1016/j.apr.2018.08.009, 2019.

Alldredge, A. L. and Jackson, G. A.: Aggregation in marine systems: preface, Deep-Sea Res. Pt. II, 42, 1–7, https://doi.org/10.1016/0967-0645(95)90003-9, 1995.

Bartlett, K. S.: Dust Storm Forecasting For Al Udeid Ab, Qatar: An Empirical Analysis, MS thesis, Air University, Islamabad, 2004.

Behrooz, R. D., Esmaili-Sari, A., Bahramifar, N., and Kaskaoutis, D. G.: Analysis of the TSP, PM_{10} concentrations and water-soluble ionic species in airborne samples over Sistan, Iran during the summer dusty period, Atmos. Pollut. Res., 8, 403–417, 2017.

Berger, C. J. M., Lippiatt, S. M., Lawrence, M. G., and Bruland, K. W.: Application of a chemical leach technique for estimating labile particulate aluminum, iron, and manganese in the Columbia River plume and coastal waters off Oregon and Washington, J. Geophys. Res.-Oceans, 113, C00B01, https://doi.org/10.1029/2007JC004703, 2008.

Brewer, P. G. and Dyrssen, D.: Chemical Oceanography of the Persian Gulf, Prog. Oceanog., 14, 41–55, 1985.

Bruland, K. W. and Franks, R. P.: Mn, Ni, Cu, Zn and Cd in the Western North Atlantic, in: Trace Metals in Seawater, edited by: Wong, C. S., Boyle, E., Bruland, K. W., Burton, J. D., and Goldberg, E. D., Plenum Press, New York, 395–414, 1983.

Bruland, K. W., Donat, J. R., and Hutchins, D. A.: Interactive influences of bioactive trace metals on biological production in oceanic waters, Limnol. Oceanogr., 36, 1555–1577, 1991.

Bu-Olayan, A. H., Al-Hassan, R., Thomas, B. V., and Subrahmanyam, M. N. V.: Impact of trace metals and nutrients levels on phytoplankton from the Kuwait Coast, Environ. Int., 26, 199–203, 2001.

Collier, R. and Edmond, J.: The trace element geochemistry of marine biogenic particulate matter, Prog. Oceanogr., 13, 113–199, 1984.

Cutter, G. A., Andersson, P., Codispoti, L., Croot, P., Francois, F., Lohan, M. C., Obata, H., and Rutgers van der Loeff, M.: Sampling and Sample-handling Protocols for GEOTRACES Cruises, available at: http://www.geotraces.org/libraries/documents/Intercalibration/Cookbook.pdf (Cookbook, version 3.0, last access: 2017), 178 pp., 2010.

Dammshauser, A., Wagener, T., Garbe-Schönberg, D., and Croot, P.: Particulate and dissolved aluminum and titanium in the upper water column of the Atlantic Ocean, Deep-Sea Res. Pt. I, 73, 127–139, 2013.

Doney, S., Fabry, V., Feely, R., and Kleypas, J.: Ocean acidification: the other CO_2 problem, Ann. Rev. Mar. Sci., 1, 169–192, 2009.

Dorgham, M. M.: Plankton research in the ROPME Sea Area, Achievements and Gaps, Int. J. Environmental Res., 7, 767–778, 2013.

Ho, T. Y., Quigg, A., Finkel, Z. V., Milligan, A. J., Wyman, K., Falkowski, P. G., and Morel, F. M.: The elemental composition of some marine phytoplankton, J. Phycol., 39, 1145–1159, 2003.

Ho, T. Y., Wen, L. S., You, C. F., and Lee, D. C.: The trace-metal composition of size-fractionated plankton in the South China Sea: Biotic versus abiotic sources, Limnol. Oceanogr., 52, 1776–1788, 2007.

Iwamoto, Y. and Uematsu, M.: Spatial variation of biogenic and crustal elements in suspended particulate matter from surface waters of the North Pacific and its marginal seas, Prog. Oceanogr., 126, 211–223, 2014.

Jeandel, C., Caisso, M., and Minster, J. F.: Vanadium behavior in the global ocean and in the Mediterranean Sea, Marine Chem., 21, 51–74, 1987

Jish Prakash, P., Stenchikov, G., Kalenderski, S., Osipov, S., and Bangalath, H.: The impact of dust storms on the Arabian Peninsula and the Red Sea, Atmos. Chem. Phys., 15, 199–222, https://doi.org/10.5194/acp-15-199-2015, 2015.

Khudhair, A. Y., Khalaf, T. A., Ajeel, S. G., and Saad, R.: Estimation of heavy metals in zooplankton organisms of N.W. Arabian Gulf, available at: https://www.cbd.int/doc/meetings/mar/ebsaws-2015-02/other/ebsaws-2015-02-iraq-submission3-en.pdf, last access: 2015.

Knauer, G. A. and Martin, J. H.: Primary production and carbon-nitrogen fluxes in the upper 1500 m of the northeast Pacific, Limnol. Oceanogr., 26, 181–186, 1981.

Krishnaswami, S. and Sarin, M. M.: The simultaneous determination of Th, U, Ra isotopes, ^{210}Pb, ^{55}Fe, ^{32}Si, and ^{14}C in marine suspended phases, Anal. Chim. Acta, 83, 143–156, 1976.

Kuss, J. and Kremling, K.: Spatial variability of particle associated trace elements in near-surface waters of the North Atlantic derived by large-volume sampling, Marine Chem., 68, 71–86, 1999.

Lam, P. J., Ohnemus, D. C., and Auro, M. E.: Size-fractionated major particle composition and concentrations from the US GEOTRACES North Atlantic Zonal Transect, Deep-Sea Res. Pt. II, 116, 303–320, https://doi.org/10.1016/j.dsr2.2014.11.020, 2015.

Land, L. S. and Hoops, G. H.: Sodium in carbonate sediments and rocks: a possible index to the salinity of diagenetic solutions, J. Sediment. Res., 43, 614–617, 1973.

Lawrence, C. R. and Neff, J. C.: The contemporary physical and chemical flux of Aeolian dust: a synthesis of direct measurements of dust deposition, Chem. Geol., 267, 46–63, 2009.

Liao, W.-H., Yang, S.-C., and Ho, T.-Y.: Trace metal composition of size-fractionated plankton in the Western Philippine Sea: The

impact of anthropogenic aerosol deposition, Limnol. Oceanogr., 62, 2243–2259, https://doi.org/10.1002/lno.10564, 2017.

Mahowald, N. M., Baker, A. R., Bergametti, G., Brooks, N., Duce, R. A., Jickells, T. D., Kubilay, N., Prospero, J. M., and Tegen, I.: Atmospheric global dust cycle and iron inputs to the ocean, Global Biogeochem. Cycles, 19, GB4025, https://doi.org/10.1029/2004GB002402, 2005.

Martin, J. H. and Knauer, G. A.: The elemental composition of plankton, Geochim. Cosmochim. Ac., 37, 1639–1653, 1973.

Milliman, J. D.: Recent sedimentary carbonates part 1, in: Marine Carbonates, Springer-Verlag, New York, Heidelberg, Berlin, 375 pp., 1974.

Muhs, D. R., Prospero, J. M., Baddock, M. C., and Gill, T. E.: Identifying Sources of Aeolian Mineral Dust: Past and Present, in: Mineral Dust, edited by: Knippertz, P. and Stuut, J.-B. W., 51–47, 2014.

Ohnemus, D. C. and Lam, P. J.: Cycling of lithogenic marine particles in the US GEOTRACES North Atlantic transect, Deep-Sea Res. Pt. II, 116, 283–302, https://doi.org/10.1016/j.dsr2.2014.11.019, 2015.

Ohnemus, D. C., Rauschenberg, S., Cutter, G. A., Fitzsimmons, J. N., Sherrell, R. M., and Twining, B. S.: Elevated trace metal content of prokaryotic communities associated with marine oxygen deficient zones, Limnol. Oceanogr., 62, 3–25, https://doi.org/10.1002/lno.10363, 2017.

Patey, M. D., Achterberg, E. P., Rijkenberg, M. J., and Pearce, R.: Aerosol time-series measurements over the tropical Northeast Atlantic Ocean: Dust sources, elemental composition and mineralogy, Marine Chem., 174, 103–119, 2015.

Pilson, M. E. Q.: An Introduction to the Chemistry of the Sea, second edition, Cambridge University Press, UK, 524 pp., https://doi.org/10.1017/CBO9781139047203, 2013.

Polikarpov, I., Saburova, M., and Al-Yamani, F.: Diversity and distribution of winter phytoplankton in the Arabian Gulf and the Sea of Oman, Cont. Shelf Res., 119, 85–99, 2016.

Prospero, J. M., Glaccum, R. A., and Nees, R. T.: Atmospheric transport of soil dust from Africa to South America, Nature, 289, 570–572, 1981.

Quigg, A., Al-Ansi, M., Al-Din, N. N., Wei, C.-L., Nunnally, C. C., Al-Ansari, I., Rowe, G. T., Soliman, Y., Al-Maslamani, I., Mahmoud, I., Youssef, N., and Abdel-Moati, M. A.: Phytoplankton along the coastal shelf of an oligotrophic hypersaline environment in a semi-enclosed marginal sea: Qatar (Arabian Gulf), Cont. Shelf Res., 60, 1–16, 2013.

Rao, D. V. and Al-Yamani, F.: Phytoplankton ecology in the waters between Shatt Al-Arab and Straits of Hormuz, Arabian Gulf: A review, Plankton Biol. Ecol., 45, 101–116, 1998.

Rashki, A., Eriksson, P. G., Rautenbach, C. J. de W., Kaskaoutis, D. G., Grote, W., and Dykstra, J.: Assessment of chemical and mineralogical characteristics of airborne dust in the Sistan region, Iran, Chemosphere, 90, 227–236, 2013.

Rauschenberg, S. and Twining, B. S.: Evaluation of approaches to estimate biogenic particulate trace metals in the ocean, Marine Chem., 171, 67–77, 2015.

Reynolds, R. M.: Physical oceanography of the Gulf, Strait of Hormuz, and the Gulf of Oman – Results from the Mt Mitchell expedition, Mar. Pollution Bull., 27, 35–59, 1993.

Richer, R.: Conservation in Qatar: Impacts of Increasing Industrialization. Occasional Paper. Centre for International and Regional Studies, Georgetown University of Foreign Service in Qatar, p. 23, 2009.

Rudnick, R. L. and Gao, S.: Composition of the continental crust, in: The Crust, vol. 3, edited by: Rudnick, R. L., Elsevier, Amsterdam, the Netherlands, pp. 1–64, 2003.

Sadooni, F. N.: Geology of Qatar: A brief introduction, Publication of the Environmental Studies Center, Qatar University, Doha, Qatar, 36 pp., 2014.

Sañudo-Wilhelmy, S. A., Kustka, A. B., Gobler, C. J., Hutchins, D. A., Yang, M., Lwiza, K., Burns, J., Capone, D. G., Raven, J. A., and Carpenter, E. J.: Phosphorus limitation of nitrogen fixation by Trichodesmium in the central Atlantic Ocean, Nature, 411, 66–69, 2001.

Schlitzer, R.: Ocean Data View, available at: http://odv.awi.de (last access: 28 October 2019, ODV Version: ODV 5.2.0), 2018.

Swift, S. A. and Bower, A. S.: Formation and circulation of dense water in the Persian/Arabian Gulf, J. Geophys. Res., 108, https://doi.org/10.1029/2002JC001360, 2003.

Turekian, K. K.: The fate of metals in the oceans, Geochim. Cosmochim. Ac. 41, 1139–l144, 1977.

Twining, B. S., Baines, S. B., Fisher, N. S., Maser, J., Vogt, S., Jacobsen, C., Tovar-Sanchez, A., and Sañudo-Wilhelmy, S. A.: Quantifying trace elements in individual aquatic protest cells with a synchrotron X-ray fluorescence microprobe, Anal. Chem., 75, 3806–3816, 2003.

Twining, B. S., Baines, S. B., and Fisher, N. S.: Element stoichiometries of individual plankton cells collected during the Southern Ocean Iron Experiment (SOFeX), Limnol. Oceanogr., 49, 2115–2128, 2004.

Twining, B. S., Baines, S. B., Vogt, S., and de Jonge, M. D.: Exploring ocean biogeochemistry by single-cell microprobe analysis of protist elemental composition, J. Eukaryot. Microbiol., 55, 151–162, 2008.

Twining, B. S., Baines, S. B., Bozard, J. B., Vogt, S., Walker, E. A., and Nelson, D. M.: Metal quotas of plankton in the equatorial Pacific Ocean, Deep-Sea Res. Pt. II, 58, 325–341, 2011.

Yigiterhan, O. and Murray, J. W.: Trace metal composition of particulate matter of the Danube River and Turkish rivers draining into the Black Sea, Marine Chem., 111, 63–76, 2008.

Yigiterhan, O., Murray, J. W., and Tuğrul, S.: Trace metal composition of suspended particulate matter in the water column of the Black Sea, Marine Chem., 126, 207–228, 2011.

Yigiterhan, O., Alfoldy, B. Z, Giamberini, M., Turner, J. C., Al-Ansari, E. S., Abdel-Moati, M. A., Al-Maslamani, I. A., Kotb, M. M., Elobaid, E. A., Hassan, H. A., Obbard, J. P., and Murray, J. W.: Geochemical Composition of Aeolian Dust and Surface Deposits from the Qatar Peninsula, Chem. Geol., 476, 24–45, 2018.

Yigiterhan, O., Al-Ansari, E. M., Nelson, A., Abdel-Moati, M. A., Turner, J., Alsaadi, H. A., Paul, B., Al-Maslamani, I. A., Al-Ansi, A.-Y. M. A., and Murray, J. W.: Trace Element Composition of Plankton from the Qatari Exclusive Economic Zone (EEZ) of the Arabian Gulf, SEANOE, https://doi.org/10.17882/71591, 2020.